# Triphenylethanamine Derivatives as Cholesteryl Ester Transfer Protein Inhibitors: Discovery of N-[(1R)-1-(3-Cyclopropoxy-4-fluorophenyl)-1-[3-fluoro-5-(1,1,2,2-tetrafluoroethoxy)phenyl]-2-phenylethyl]-4-fluoro-3-(trifluoromethyl)benzamide (BMS-795311)

Jennifer X. Qiao,[*,†] Tammy C. Wang,[†] Leonard P. Adam,[‡] Alice Ye A. Chen,[‡] David S. Taylor,[‡] Richard Z. Yang,[‡] Shaobin Zhuang,[‡] Paul G. Sleph,[‡] Julia P. Li,[§] Danshi Li,[§] Xiaohong Yin,[‡] Ming Chang,[∥] Xue-Qing Chen,[⊥] Hong Shen,[∥] Jianqing Li,[†] Daniel Smith,[†] Dauh-Rurng Wu,[†] Leslie Leith,[†] Lalgudi S. Harikrishnan,[†] Muthoni G. Kamau,[†] Michael M. Miller,[†] Donna Bilder,[†] Richard Rampulla,[†] Yi-Xin Li,[∥] Carrie Xu,[∥] R. Michael Lawrence,[†] Michael A. Poss,[†] Paul Levesque,[§] David A. Gordon,[‡] Christine S. Huang,[∥] Heather J. Finlay,[†] Ruth R. Wexler,[†] and Mark E. Salvati[†]

Departments of [†]Discovery Chemistry, [‡]Discovery Biology, [§]Discovery Toxicology, [∥]Preclinical Candidate Optimization, and [⊥]Pharmaceutics, Bristol-Myers Squibb Company, Research and Development, P.O. Box 4000, Princeton, New Jersey 08543-4000, United States

Ⓢ *Supporting Information*

ABSTRACT: Cholesteryl ester transfer protein (CETP) inhibitors raise HDL-C in animals and humans and may be antiatherosclerotic by enhancing reverse cholesterol transport (RCT). In this article, we describe the lead optimization efforts resulting in the discovery of a series of triphenylethanamine (TPE) ureas and amides as potent and orally available CETP inhibitors. Compound **10g** is a potent CETP inhibitor that maximally inhibited cholesteryl ester (CE) transfer activity at an oral dose of 1 mg/kg in human CETP/apoB-100 dual transgenic mice and increased HDL cholesterol content and size comparable to torcetrapib (**1**) in moderately-fat fed hamsters. In contrast to the off-target liabilities with **1**, no blood pressure increase was observed with **10g** in rat telemetry studies and no increase of aldosterone synthase (CYP11B2) was detected in H295R cells. On the basis of its preclinical profile, compound **10g** was advanced into preclinical safety studies.

10g
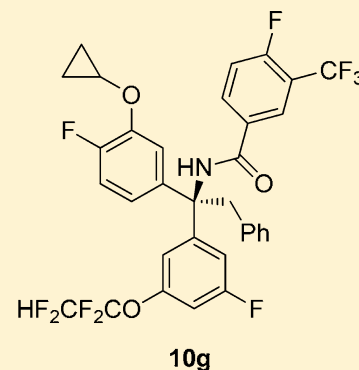
INTRODUCTION

Cardiovascular (CV) disease remains the leading cause of morbidity and mortality worldwide. In addition to high levels of low density lipoprotein-cholesterol (LDL-C), low levels of high density lipoprotein-cholesterol (HDL-C) are known to be an independent risk factor for coronary heart disease (CHD) based on epidemiological studies.[1] Cholesteryl ester transfer protein (CETP) is a plasma glycoprotein that is responsible for transporting neutral lipids such as cholesteryl esters (CEs) and triglycerides (TGs) among various classes of lipoproteins including HDL, LDL, and very low density lipoprotein (VLDL).[2] Physiologically, CETP facilitates the transfer of CE from HDL to LDL and VLDL in exchange for TG, leading to decreased HDL-C levels and increased LDL-C levels. Preclinical animal models and clinical data with four CETP inhibitors (Figure 1A), torcetrapib (**1**), dalcetrapib (**2**), anacetrapib (**3**), and evacetrapib (**4**), demonstrate an elevation of plasma HDL-C and a reduction of plasma LDL-C levels associated with CETP inhibition.[3] An increased level of HDL-C by CETP inhibition is potentially beneficial for patients with CHD due to an increase in reverse cholesterol transport

(RCT), i.e., the transport of cholesterol from peripheral tissues (e.g., the atherosclerotic plaque) to the liver for disposal from the body.[4] In addition to invoking a significant increase in HDL-C, CETP inhibitors such as compounds **3** and **4** have also been shown to lower LDL and lipoprotein(a) (Lp(a)) levels that could potentially contribute to a reduction of atherosclerosis.[5] Although the known effects of CETP inhibition on plasma lipoproteins, i.e., profound elevation of HDL-C levels as well as lowering LDL-C levels, are considered positive, the effects on morbidity and mortality in CHD patients are still being evaluated in late-stage clinical trials with compounds **3** and **4**. Compound **1**, on the other hand, was abruptly terminated in the ILLUMINATE phase III trial in 2006 after a little more than a year of treatment due to an unacceptable mortality increase in the **1** plus atorvastatin group versus the atorvastatin group alone.[6] The increased mortality is now widely believed to be due to adverse off-target effects including a significant increase of blood pressure (BP)[6b,c] and aldosterone
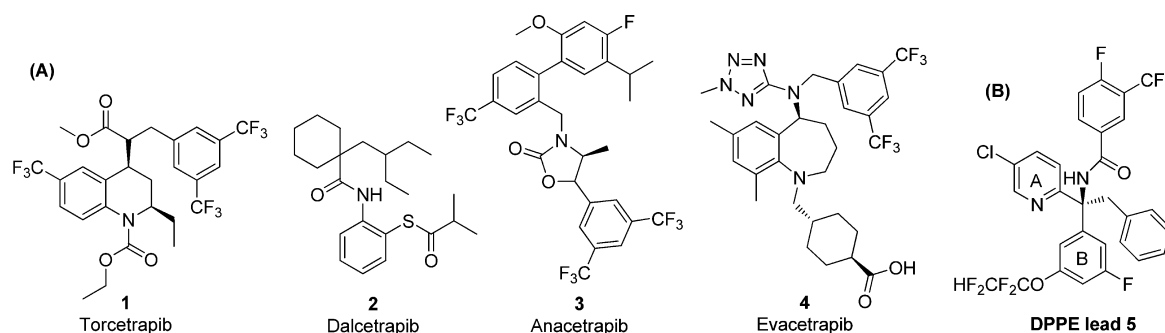
Figure 1. (A) CETP inhibitors **1**−**4** that have entered phase III clinical trials. (B) Diphenylpyridylethanamine (DPPE) lead **5**.

levels.[6d,e] Clinical studies with compound **2**, a weak and covalent inhibitor of CETP, were terminated in 2011 due to the lack of clinical efficacy in the reduction of CV events.[7]

We previously disclosed a series of diphenylpyridylethanamine (DPPE) derivatives that resulted in the optimized lead **5** bearing a 4-chloro-2-pyridyl A-ring (Figure 1B) as a potent CETP inhibitor.[8a] The in vitro CETP inhibitory activity of **5** was 36 nM in an enzyme-based scintillation proximity assay (SPA).[8a,9] In a human whole plasma assay (hWPA),[8a] an assay that measures the transfer of [^{3}H]CE from HDL to LDL in about 95% human plasma, **5** had an IC$_{50}$ of 3.6 μM, 100-fold right-shifted from the SPA IC$_{50}$. The hWPA is thought to be more predictive of in vivo activity than the SPA because it takes into consideration plasma protein binding. At the time of optimization of the DPPE series, compound **1** was in a phase IIb clinical trial and was selected as the benchmark compound for our studies, while structures and activity profiles of **3** and **4** have been disclosed only at later time points. Compound **1** was more potent than **5** in both the SPA and the hWPA assays (SPA IC$_{50}$ = 2.7 nM, hWPA IC$_{50}$ = 0.10 μM). Nevertheless, sufficient plasma exposures of **5** could be achieved which resulted in inhibition of CETP-mediated CE transfer in human CETP/apoB-100 (hCETP/apoB-100) dual transgenic (Tg) mice[8a,10] and an elevation of plasma HDL-C levels in moderately fat fed hamsters.[8a,11] The goal of this work was to identify a more potent compound than **5** that had excellent plasma exposures upon oral dosing, improved pharmacodynamic effects (similar to **1**) and did not possess known off-target effects (e.g., BP increase in animals). Initially, with the identification of **5**, various A-ring analogs were surveyed in an effort to identify compounds with improved hWPA CETP inhibitory potency with the hope that this would translate into enhanced reduction of CE transfer activity in vivo and elevation of HDL-C at lower doses.

It was previously believed that the pyridine nitrogen in the A-ring of **5** was critical for potency.[8a] This was based on the early ester series obtained from virtual screening, in which the phenyl A-ring analog **6b** was much less potent in the hWPA than the corresponding 2-pyridyl analog **6a** (Table 1). In search of diverse monocyclic A-rings other than the 2-pyridyl group, we found that hWPA potency was sensitive to the polarity of the heterocyclic A-ring. Polar heteroaryls such as pyridinones, imidazoles, and pyrazines were not tolerated, while relatively nonpolar heteroaryls such as thiazoles and furans exhibited potency similar to the 2-pyridyl A-ring analogs.[8a,12] We also found that the meta substituted CF$_3$ group in **7b** improved hWPA activity similar to that previously observed for the para-chloropyridyl A-ring in **5** (Table 1). However, the isomeric pyridine **7a** was much less potent. Although the trifluoromethyl

**Table 1. Evolution of the First Triphenylethanamine (TPE) Derivative: Phenyl A-Ring Analog 8a**[a]

| compd	X	Y	CETP SPA IC$_{50}$ (nM)	CETP hWPA IC$_{50}$ (μM)
6a	N		1300 ± 800 (n = 3)	9.4 ± 1.8 (n = 2)
6b	CH		4200 ± 2700 (n = 3)	53, >100
7a	N	CH	760 ± 200 (n = 2)	29 ± 0.2 (n = 2)
7b	CH	N	24 ± 12 (n = 3)	2.2 ± 0.9 (n = 5)
7c	N	N	60	23
8a	CH	CH	12	1.5 ± 0.5 (n = 3)
5			36 ± 15 (n = 7)	3.6 ± 2.8 (n = 7)
1			2.7 ± 0.9 (n = 183)	0.10 ± 0.05 (n = 248)

[a]Compound inhibition in the SPA and hWPA was measured in duplicate at six concentrations, and the mean values were used to calculate the IC$_{50}$. IC$_{50}$ values are reported as the mean ± SD for $n \geq$ 2. See ref 8a and Supporting Information for details.

group in **7a** might be making favorable interactions with the protein, its adjacent pyridyl nitrogen atom (X = N) may be buried in an energy penalizing hydrophobic environment. Conversely, the pyridyl nitrogen atom (Y = N) in **7b** may be more solvent exposed; thus N and CH at this position may be interchangeable. Compound **7c** bearing a more polar pyrimidine A-ring (X = Y = N) exhibited a decrease in hWPA activity. The observed A-ring SAR prompted us to investigate nonpolar phenyl A-ring analogs. We were gratified that the first phenyl A-ring analog **8a**, a triphenylethanamine (TPE) derivative containing a meta CF$_3$ group, was equipotent to the corresponding aza analog **7b** in both the SPA and the hWPA. At the time of the research, there was no CETP structural information available. Structure-based design was therefore not used in the lead optimization process.

In this paper, we shall discuss optimization efforts on the phenyl A-ring of **8a**, which resulted in the identification of a series of potent and orally bioavailable TPE amides and ureas with improved hWPA activity. These compounds showed improved pharmacodynamic effects in terms of both CE transfer inhibition and HDL elevation as compared with **5**. Furthermore, we demonstrate with a large set of TPE analogs that there are strong correlations between the in vitro hWPA potency and metabolic stability and in vivo inhibition of CE transfer in Tg mice. Throughout our studies, the in vitro hWPA potency and stability profile were used to guide compound

Scheme 1[a]
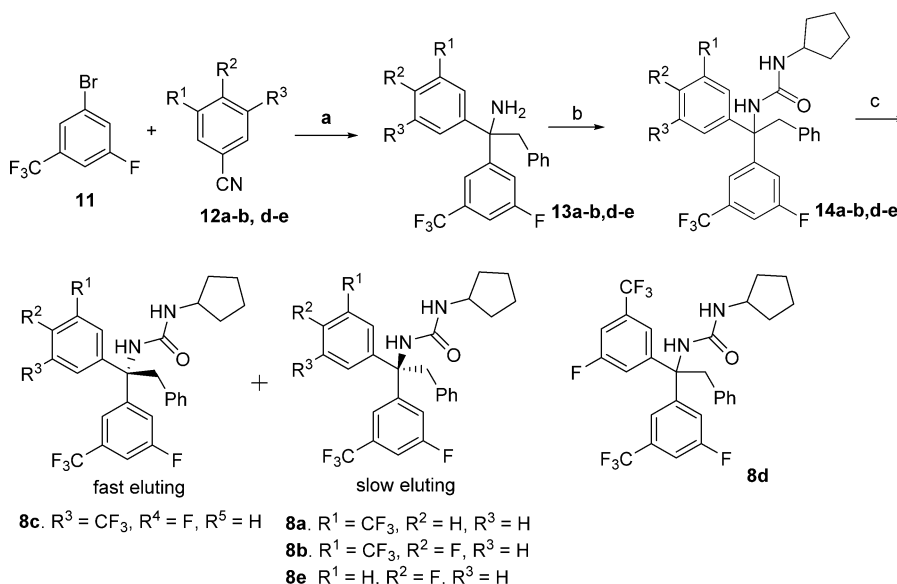
[a]Reagents and conditions: (a) *n*-BuLi (2.5 M in hexanes, 1.1 equiv), Et$_2$O, −78 °C, 30 min, 4-fluoro-3-(trifluoromethyl)benzonitrile (1.0 equiv), −78 °C, 2 h, TMSCl, THF, −78 °C to rt, 2 h; BnMgBr (2.0 M in THF, 2 equiv), −78 °C to rt, 16 h, 1 N HCl, 19−87%; (b) NCO-cyclopentyl, 1,4-dioxane, 16 h, 55−67%; (c) chiral preparative HPLC, AD column (10% isopropanol/heptane/0.1% DEA, isocratic); **8c**, fast eluting, 44%; **8b**, slow eluting, 42%.

Scheme 2[a]
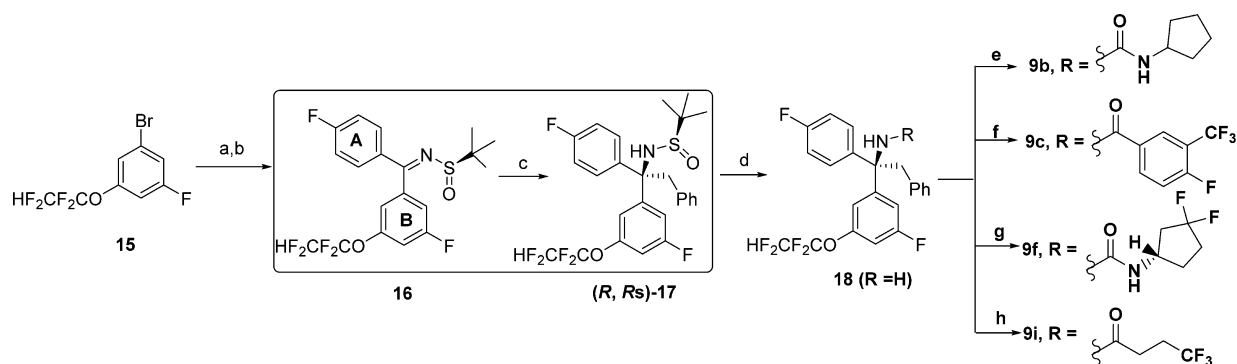
[a]Reagents and conditions: (a) *n*-BuLi, 4-fluorobenzonitrile, Et$_2$O, −78 °C, then 1 N HCl, 87%; (b) (*R*)-(+)-2-methylpropane-2-sulfinamide, Ti(OEt)$_4$, THF, reflux, 81%; (c) BnMgBr (1.0 M in Et$_2$O, 2 equiv), BF$_3$·Et$_2$O (2 equiv), −78 °C, 1.5 h, CH$_2$Cl$_2$, dr (*R*,*R*s)-**17**/(*S*,*R*s)-**17** = 5.3:1, isolated yield for (*R*,*R*s)-**17**, 81%; (d) 4 N HCl in dioxane, MeOH, 82%; (e) NCO-cyclopentyl, CH$_2$Cl$_2$, rt, 16 h, 70%; (f) 4-fluoro-3-(trifluoromethyl)benzoyl chloride, Et$_3$N, CH$_2$Cl$_2$, rt, 5 h, 95%; (g) *p*-nitrophenyl chloroformate, K$_2$CO$_3$, THF, rt; then (1*S*)-3,3-difluorocyclopentan-1-amine,[8b] DIPEA, CH$_2$Cl$_2$, rt, 16 h, SFC separation, 35%; (h) 4,4,4-trifluorobutanoic acid, PyBOP, *N*-methylmorpholine, CH$_2$Cl$_2$, rt, 8 h, 66%.

selection for Tg mouse studies. After achieving a compound-**1**-like PD response, we investigated the effect on BP of the lead compounds in telemeterized rats, which guided our efforts to focus on further modifications on the 4-fluoro-3-substituted phenyl A-rings in the N-terminus arylamide series. This ultimately led to the discovery of our first preclinical candidate BMS-795311 (compound **10g**). The in vitro and in vivo activity and liability profile of **10g** will be described.

■ RESULTS AND DISCUSSION

Chemistry. Schemes 1−6 illustrate the synthesis of compounds described herein. To construct the requisite tertiary carbinamines of TPE analogs, we adapted two general synthetic strategies that had previously been disclosed for the DPPE series.[8a,13] In the first method, racemic tertiary amines were obtained by the addition of benzyl Grignard to the TMSCl-

activated imines derived from the corresponding arylnitriles and the aryllithium species, followed by removal of the labile TMS group in a one-pot three-component reaction. Scheme 1 illustrates the initial synthesis of TPE ureas **8a−e** from 3-fluoro-5-trifluoromethylphenyl bromide (**11**) and the corresponding A-ring nitriles **12**. Unlike the formation of DPPE carbinamines, an additional equivalent of benzylmagnesium bromide, a higher temperature, and a longer reaction time (stirring the mixture at room temperature overnight) were necessary in order to obtain the TPE carbinamines in good yields at the Grignard addition step. The racemic mixture of ureas **14** was separated via chiral HPLC. The desired enantiomers **8a**, **8b**, and **8e** eluted much slower than the corresponding undesired enantiomer (e.g., **8c**).

Since the in vitro potency of the TPE derivatives resided in only one enantiomer, we then used Ellman's *tert*-butanesulfi-namide chemistry to generate the desired TPE tertiary

Scheme 3[a]
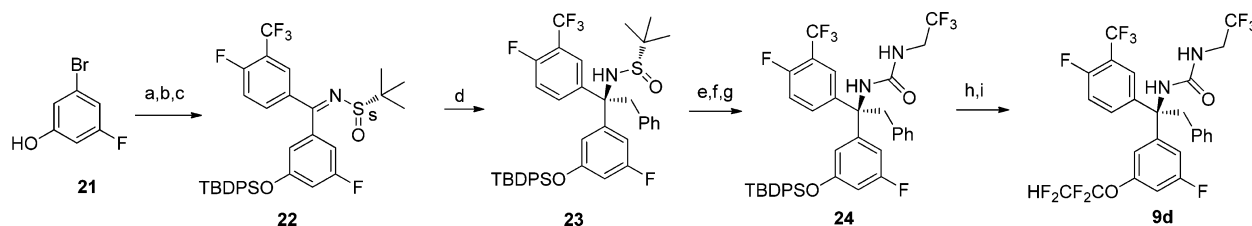
[a]Reagents and conditions: (a) tert-butyldiphenylsilyl chloride, imidazole, 0 °C to rt, 18 h, 58%; (b) n-BuLi (2.5 M in hexanes, 1.1 equiv), Et$_2$O, −78 °C, 30 min; 4-fluoro-3-trifluoromethylbenzonitrile, −78 °C, 1.5 h; 1 N HCl, 79%; (c) (S)-(−)-2-methylpropane-2-sulfinamide, Ti(OEt)$_4$, THF, reflux, 83%; (d) BF$_3$·Et$_2$O (2 equiv), BnMgCl in Et$_2$O (2.8 equiv), CH$_2$Cl$_2$, −78 °C, dr, (R,Ss)-23/(S,Ss)-23 = 5:1, yield for (R,Ss)-23, 62%; (e) 4 N HCl dioxane/MeOH; (f) isopropenyl chloroformate, K$_2$CO$_3$, THF/H$_2$O, rt, 4 h; (g) NH$_2$CH$_2$CF$_3$, N-methylpyrrolidine (cat.), THF/DMSO, microwave irradiation, 180 °C, 20 min, 82% for 3 steps; (h) TBAF, THF, 0 °C, 45 min, 77%; (i) ICF$_2$CF$_2$H, K$_2$CO$_3$, DMSO, 70 °C, 16 h, 58%.

Scheme 4[a]
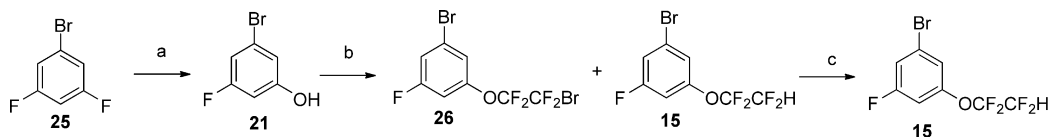
[a]Reagents and conditions: (a) KOSiMe$_3$ (3.5 equiv), diglyme, 120 °C, 5 h, 92%; (b) BrCF$_2$CF$_2$Br, DMSO, Cs$_2$CO$_3$ (1.5 equiv), 50 °C, 5 h, 94%; (c) Zn, HOAc, 50 °C, 1 h, 87%.

Scheme 5[a]
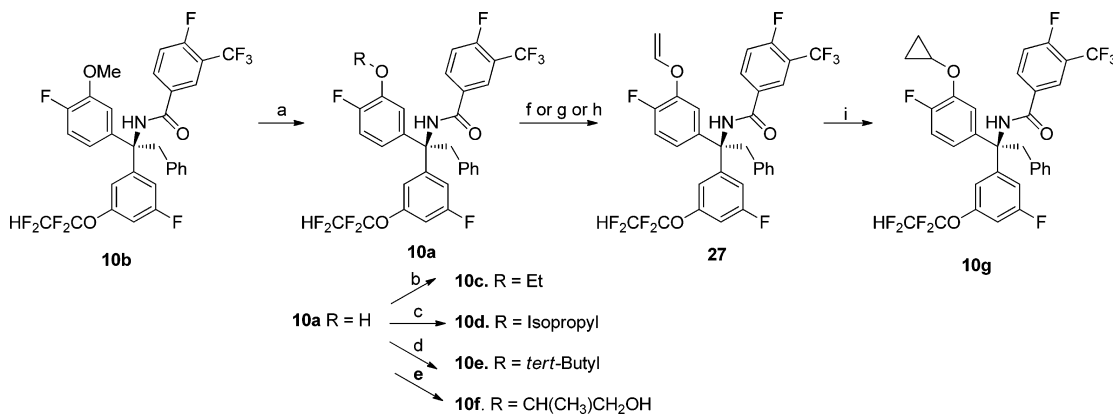
[a]Reagents and conditions: (a) BBr$_3$, CH$_2$Cl$_2$, 0 °C to rt, 2 h, 100%; (b) ethyl iodide, K$_2$CO$_3$, 50 °C, DMF, 90%; (c) isopropyl iodide, K$_2$CO$_3$, DMF, 60 °C, 16 h, 86%; (d) 1,1-di-tert-butoxy-N,N-dimethylmethanamine, DMF, 110 °C, 5 h, 81%; (e) ethyl 2-bromopropanoate, K$_2$CO$_3$, rt, 16 h, then NaBH$_4$, THF, 0 °C to rt, 16 h, 27% for 2 steps; (f) 2,4,6-trivinylcyclotriboroxane−pyridine complex, Cu(OAc)$_2$, pyridine, CH$_2$Cl$_2$, rt, 2 days, 93%; (g) ethenyl acetate, [Ir(COD)Cl]$_2$, Na$_2$CO$_3$, toluene, 100 °C, 77%; (h) 2-chloroethyl 4-methylbenzene-1-sulfonate (1.75 equiv), Cs$_2$CO$_3$ (1.1 equiv), Triton X-405 (5% w/w), THF; KO-t-Bu (5 equiv), 0−7 °C, 76−80% for 2 steps; (i) Et$_2$Zn, TFA, CH$_2$I$_2$, CH$_2$Cl$_2$, −10 °C to rt, 78−83%.

carbinamines via the addition of benzyl Grignard to the N-tert-butanesulfinyl ketimines derived from the corresponding diaryl ketones followed by the separation of the diastereomers using silica gel chromatography and removal of the tert-butanesulfinyl group (second general method).[8a,13] In large-scale syntheses, the diastereomeric mixtures were separated by supercritical fluid chromatography (SFC). Scheme 2 illustrates the synthesis of 9b, 9c, 9f, and 9i bearing the 4-fluorophenyl A-ring and the 3-fluoro-5-tetrafluoroethyl ether phenyl B-ring. The benzylic protons (CH$_a$H$_b$Ph) of the two diastereomers (R,Rs)-17 and (S,Rs)-17 showed a distinctive AA′BB′ pattern in the 1D proton NMR. The chemical shifts of CH$_a$H$_b$ of the desired diastereomer (R,Rs)-17 were more separated than the other isomer (S,Rs)-17. Therefore, we used the integration of the CH$_a$H$_b$Ph protons of the crude reaction mixture to determine the diastereomeric ratio (dr) of the Grignard reaction (step c in

Scheme 2). The temperature, solvent, concentration, and additive effects on the dr of the Grignard addition step were investigated. The noncoordinating solvents such as CH$_2$Cl$_2$ gave better dr, suggesting a favorable chelated six-membered cyclic TS[‡].[14] Single crystal X-ray crystallography confirmed the absolute stereochemistry of the major diastereomer as (R,Rs)-17.[15] Due to the absence of hetero ring atoms on the A- or B-rings, Lewis acid additives, such as BF$_3$·Et$_2$O did not improve dr; however, the reaction generally proceeded faster with Et$_2$O·BF$_3$ than without Et$_2$O·BF$_3$. The best conditions utilized 2 equiv of BF$_3$·Et$_2$O in CH$_2$Cl$_2$ at −78 °C with 2.1−3.5 equiv of BnMgCl and gave an 84% isolated yield of the desired isomer (R,Rs)-17 after column chromatography separation. Urea or amide formation from 18 then provided the desired compounds 9b, 9c, 9f, and 9i.

Scheme 6[a]
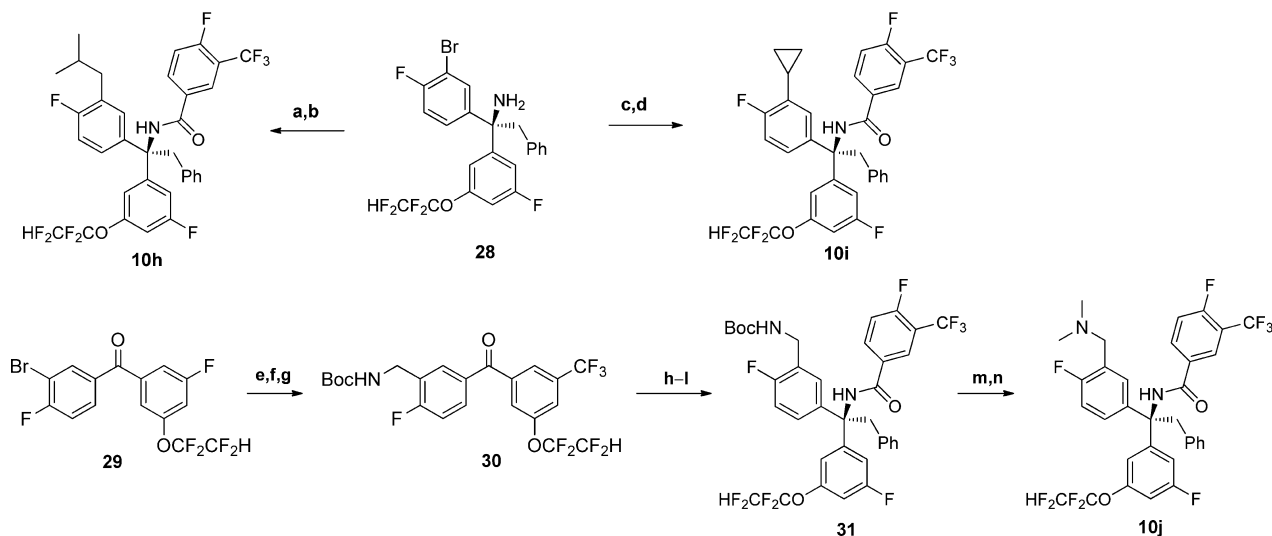
[a]Reagents and conditions: (a) PEPPSI-IPr (0.2 equiv), isobutylzinc(II) bromide (6 equiv), NMP, THF, 75 °C, 2 h, rt, 3 days, 36%; (b) 4-fluoro-3-(trifluoromethyl)benzoyl chloride, Na$_2$CO$_3$, THF, rt, 2 h, 48%; (b) cyclopropylboronic acid, palladium(II) acetate (5 mol %), tricyclohexylphosphine (10 mol %), K$_3$PO$_4$, toluene, 100 °C, microwave irradiation, 15 min, 30%; (d) 1,1-di-*tert*-butoxy-*N*,*N*-dimethylmethanamine; (e) Zn(CN)$_2$, Pd(PPh$_3$)$_4$, DMF, 175 °C, 90%; (f) NaBH$_4$, NiCl$_2$, Boc$_2$O, MeOH, 0 °C to rt, 6 h, 85%; (g) Dess–Martin periodinane, CH$_2$Cl$_2$/H$_2$O, rt, 3 h, 33%; (h) (*R*)-(+)-2-methylpropane-2-sulfinamide, Ti(OEt)$_4$, THF, 75 °C, 16 h, 58%; (i) BF$_3$·OEt$_2$ (2 equiv), BnMgCl (3 equiv), CH$_2$Cl$_2$, −78 °C to rt, 3 h; (j) 4 N HCl, dioxane/MeOH; (k) (Boc)$_2$O, DIEA, CH$_2$Cl$_2$, 0 °C, 1.5 h, 72% for 3 steps; (l) 4-fluoro-3-(trifluoromethyl)benzoyl chloride, Et$_3$N, CH$_2$Cl$_2$, 0 °C to rt, 16 h, 91%; (m) 1 N HCl/Et$_2$O, CH$_2$Cl$_2$, rt, 2 h; (n) formaldehyde, NaCNBH$_3$, AcOH, MeOH, rt, 1 h, 33% for two steps.

The dr of the Grignard adducts (i.e., (*R*,*Rs*):(*S*,*Rs*)) bearing different A-ring and B-ring substituents ranged from 1:1 to 9:1. When the A-ring was 3-trifluoromethyl-4-fluorophenyl and the B-ring was 3-fluoro-5-tetrafluoroethyl ether phenyl, the route in Scheme 2 only offered a 1:1 mixture of diastereomers, which were difficult to separate by column chromatography. Because 9d was one of the most advanced compounds in the program, we optimized the tertiary carbinamine synthesis by changing the tetrafluoroethyl ether substituent on the B-ring to a *tert*-butyldiphenylsilyl ether (OTBDPS) group and switching the (*R*)-sulfamine reagent to the (*S*)-sulfamine (compound 22). Grignard addition of benzylmagnesium chloride to 22 provided an improved dr (5:1) in favor of the desired isomer (*R*,*Ss*)-23, which was the fast eluant by column chromatography (Scheme 3). Deprotection of 23 and urea formation by reaction of the intermediate isopropenyl carbamate with trifluoroethylamine gave urea 24. Removal of the TBDPS group in 24 followed by alkylation of the resulting phenol with tetrafluoroiodoethane afforded 9d.
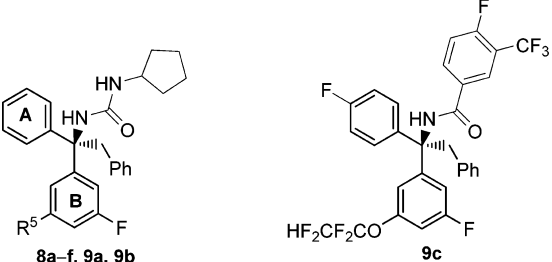
To access kilogram quantities of the optimal B-ring bromide 15, we developed a practical synthesis of 3-bromo-5-fluorophenol (21) that involved nucleophilic substitution of the readily available 3,5-difluorobromobenzene (25) with potassium trimethylsilanoate (Scheme 4).[16] Nucleophilic substitution of 1,2-dibromotetrafluoroethane with phenol 21 gave a mixture of 26 and 15 (26/15 = 95:5), which was subsequently reduced with zinc dust to provide the B-ring intermediate 15.[17]
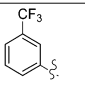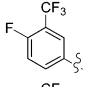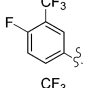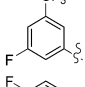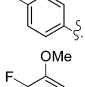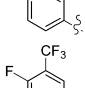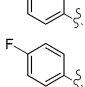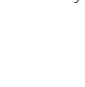
Scheme 5 illustrates the synthesis of 3-alkyl ether-4-fluorophenyl analogs 10a−11g starting from the methoxy ether 10b. Compound 10b was synthesized following the procedures described in Scheme 2. Removal of the methyl group in 10b followed by alkylation with either ethyl iodide or isopropyl iodide provided 10c and 10d, respectively. The *tert*-

butyl ether 10e was obtained by heating 10a in the presence of 1,1-di-*tert*-butoxy-*N*,*N*-dimethylmethanamine in DMF. Initially, the cyclopropyl ether 10g was synthesized via formation of the vinyl ether 27 using either Cu(OAc)$_2$-mediated C−O coupling of phenol 10a with trivinylcyclotriboroxane−pyridine complex[18a] or iridium-catalyst transfer vinylation of phenol 10a with vinyl acetate,[18b] followed by Simmons−Smith cyclopropanation of 27 with diiodomethane and diethylzinc in the presence of trifluoroacetic acid. In large-scale syntheses, to avoid heavy metal usage close to the end of the synthetic route, the vinyl ether 27 was prepared in a two-step nucleophilic addition and then elimination process using Cs$_2$CO$_3$ as the base for the addition step and *t*-BuOK as the base for the elimination step.

3-Isobutyl-4-fluorophenyl A ring analog 10h and 3-cyclopropyl-4-fluorophenyl A ring analog 10i were obtained from the corresponding bromide intermediate 28 (Scheme 6). Negishi coupling of 28 with isobutylzinc bromide using PEPPSI-IPr as the catalyst followed by amide formation gave 10h. Amide formation of 28 followed by Suzuki coupling with cyclopropylboronic acid afforded 10i. The synthesis of the methyldimethylamine analog 10j started with the bromobenzophenone intermediate 29. Nitrile formation followed by double reduction of the cyano group and ketone group, protection of the amine, and then Dess−Martin oxidation provided the ketone intermediate 30. Following similar procedures as shown in Scheme 2, the Boc-protected arylamide 31 was obtained. Removal of the Boc group and subsequent reductive amination afforded 10j.

Medicinal Chemistry Lead Optimization of TPE Series: Discovery of Compound 10g. The aforementioned TPE urea 8a bearing the 3-trifluoromethylphenyl A-ring in combination with the 3-trifluoromethyl-5-fluorophenyl B-ring exhibited an IC$_{50}$ of 12 nM in the SPA and 1.5 μM in the hWPA. Continued SAR studies on phenyl A-ring substitution

Table 2. In Vitro CETP Inhibitory Activity of Phenyl A-Ring Analogs[a]

Compd	A-ring	R[5] of B-ring	CETP SPA IC$_{50}$ (nM)	CETP hWPA IC$_{50}$ (μM)
8a		CF$_3$	12	1.5±0.52 (n=3)
8b		CF$_3$	4.9±1.1 (n=3)	0.38±0.20 (n=4)
8c (S)-enantiomer of 8b		CF$_3$	510±150 (n=2)	27±3.6 (n=2)
8d		CF$_3$	114	9.0
8e		CF$_3$	4.7	0.59±0.06 (n=2)
8f		CF$_3$	3.2±1.7 (n=2)	0.27±0.04 (n=2)
9a		OCF$_2$CF$_2$H	2.7±1.0 (n=2)	0.17±0.02 (n=2)
9b		OCF$_2$CF$_2$H	1.8±0.9 (n=2)	0.23±0.08 (n=2)
9c			5.3±1.9 (n=2)	0.62±0.30 (n=3)
5			36±15 (n=7)	3.6±2.8 (n=7)
1			2.7±0.9 (n=183)	0.10±0.045 (n=248)

[a]Compound inhibition in the SPA and hWPA was measured in duplicate at six concentrations, and the mean values were used to calculate the IC$_{50}$. IC$_{50}$ values are reported as the mean ± SD for $n \geq 2$; see ref 8a and Supporting Information for details.

generated many TPE analogs, some of which are exemplified in Table 2. The *R* enantiomers were generally more potent than the corresponding *S* enantiomers (e.g., **8b** vs **8c**). Compounds with 3,4-disubstituted phenyl A-rings, such as **8b** and **8f**, showed good potency in the SPA and hWPA assays. The 4-fluorophenyl substituted analog **8e** was also potent having submicromolar hWPA potency. However, the 3-fluoro-5-trifluoromethylphenyl analog **8d** was much less potent; this was also true for other 3,5-disubstituted phenyl A-ring analogs (data not shown). After optimizing the substitution pattern of the phenyl A-ring, we replaced the 3-fluoro-5-trifluoromethyl-phenyl B-ring with the more optimal 3-fluoro-5-(1,1,2,2-tetrafluoroethoxy)phenyl present in the DPPE lead **5**. The resulting compounds **9a** and **9b** were an order of magnitude more potent than **5**, having IC$_{50}$ values that were similar to **1**. Compound **9c** bearing the same aryl amide N-terminus as that of **5** also demonstrated improved potency (hWPA = 0.62 μM) relative to **5**.

The selectivity of the TPE derivatives **8f**, **9b**, and **9c** was tested against phospholipid transfer protein (PLTP),[19] the closest family member of four to CETP, and none of them inhibited PL transfer activity up to 100 μM. In addition, these

compounds did not disrupt HDL particle integrity (altered [3H]HDL mobility) in a lipoprotein disruption assay.[20]

With the hWPA activity of several compounds approaching **1**, we next measured in vivo CETP inhibition in the primary screening model, i.e., a dual transgenic (Tg) mouse PK/PD model, in which mice expressed both human CETP and human apoB-100 (Table 3).[10] Because mice utilize non-CETP mechanisms to transfer CE, the maximal inhibition of CE transfer in the Tg mouse model due to CETP inhibition was 50−70% (i.e., 30−50% of predosing activity). The lowest dose required to maximally inhibit plasma CETP activity for 8 h was defined as the minimal efficacious dose (MED). For compound **1**, the MED was 3 mg/kg, and for compound **5**, the MED was 30 mg/kg, as determined in separate dose escalation studies.

As shown in Table 3, the cyclopentylurea analogs **9a** and **9b** offered good hWPA and TgWPA activity, but the cyclopentyl functionality resulted in poor metabolic stability[8a] (MLM rate: ~0.3 nmol min^{-1} mg^{-1}); thus, neither showed significant CETP inhibition at the 8 h time point in the Tg PK/PD studies (98% and 78% of predosing activity for **9a** and **9b**, respectively). On the other hand, despite its somewhat lower hWPA and TgWPA activity compared with **9a** and **9b**, the

Table 3. In Vivo Efficacy of TPE Derivatives in Inhibition of CE Transfer in Tg Mice[a]

9a, R = CF$_3$
9b, R = H

9c

9d, n = 1
9e, n = 2

9f, R = H
9g, R = CF$_3$

compd	hWPA IC$_{50}$ (μM)[b]	TgWPA IC$_{50}$ (μM)[c]	CETP activity in Tg mice (% of predosing activity)			plasma concentration in Tg mice (μM)			AUC$_{0-8h}$ (μM·h)	HLM/MLM rate (nmol min^{-1} mg^{-1})[d]
			2 h	4 h	8 h	2 h	4 h	8 h		
9a	0.17 ± 0.02 (n = 2)	0.12	48	60	98	0.48	0.08	0.03	1.1	0.273/0.275
9b	0.23 ± 0.08 (n = 2)	0.21 ± 0.08 (n = 2)	39	53	78	5.9	1.9	0.55	17.5	0.295/0.298
9c	0.62 ± 0.30 (n = 3)	1.3 ± 0.1 (n = 2)	35	30	30	14.5	11.6	7.0	77.0	0.000/0.000
9d	0.18 ± 0.07 (n = 11)	0.072	28	35	24	3.8	2.4	0.84	15.8	0.007/0.000
9e	0.19 ± 0.07 (n = 5)	0.19	40	29	31	3.3	2.3	0.92	19.1	0.006/0.040
9f	0.21 ± 0.10 (n = 9)	0.11	42	48	63	0.89	0.19	0.054	2.2	0.062/0.126
9g	0.30 ± 0.12 (n = 6)	0.12	31	21	35	1.7	0.55	0.14	4.9	0.038/0.048
1	0.10 ± 0.05 (n = 248)	0.16	38	33	33	2.1	0.68	0.15	6.0	0.092/0.092
5[e]	3.6 ± 2.8 (n = 7)	9.0	55[e]	48[e]	40[e]	14.5[e]	15.2[e]	9.8[e]	93[e]	0.000/0.003

[a]hCETP/apoB-100 dual Tg mice were divided into groups of n = 4 or 5. Animals were fasted for 2 h, bled, and vehicle (EtOH/Cremophor/water, 10/10/80) or test compound was orally dosed at 10 mg/kg. Mice were bled at 2, 4, and 8 h post dosing. Plasma was analyzed for CETP activity and drug exposure. Compound effects on plasma CE transfer activities at the 2, 4, and 8 h time points were determined by analysis of the activity difference between samples obtained after dosing and that of the same animal before dosing. [b]Inhibition in the hWPA was measured in duplicate at six concentrations, and the mean values were used to calculate IC$_{50}$ values, which are reported as the mean ± SD (see ref 8a and Supporting Information for details). [c]For TgWPA, see ref 21 and Supporting Information for details. [d]Microsomal metabolic rate during 10 min incubation at 0.5 μM concentration. HLM: human liver microsomes. MLM: mouse liver microsomes. [e]Dose: 30 mg/kg (po).

(A)

(B)
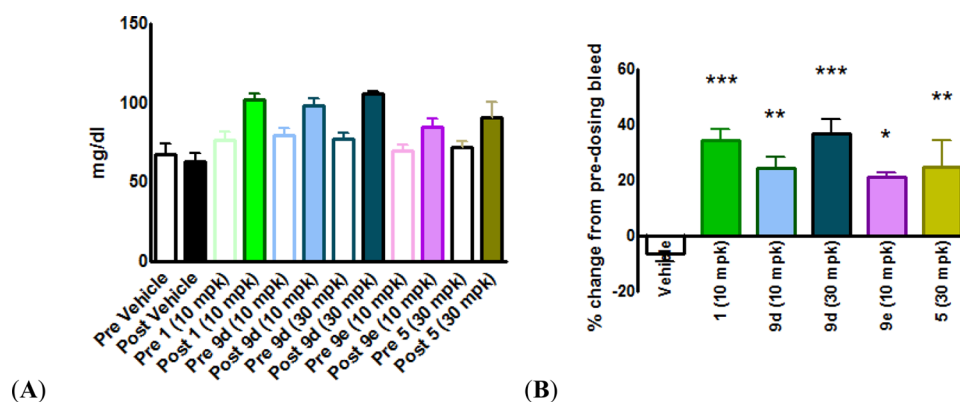
Figure 2. Elevation in HDL-C for compounds 9d, 9e, 1, and 5 in moderately fat-fed hamsters. (A) Plasma HDL-C and (B) percent changes in HDL-C after dosing compounds (po, q.d.) for 3 days. Vehicle: EtOH/Cremophor/water, 1/1/8. Plasma was obtained before dosing and 2 h after the last dose (48 h after the initiation of dosing) to determine the effects of drug treatment on HDL-C levels. HDL-C levels were measured using an automated lipid analyzer (Lipi+plus from Polymedco on a COBAS MIRA chemistry analyzer): (∗∗∗) $p < 0.001$, (∗∗) $p < 0.01$, (∗) $p < 0.05$ vs vehicle (n = 6/group).

arylamide 9c exhibited very good metabolic stability and demonstrated complete CETP inhibition during the 8 h assay period with a plasma concentration of 7 μM at the 8 h time point, 5-fold higher than the TgWPA IC$_{50}$ of 1.3 μM. In addition to the phenylamide analog 9c, we incorporated fluorinated (cyclo)alkylureas, such as trifluoroethyl, trifluoropropyl, and S-difluorocyclopentyl substituents which had previously demonstrated improved metabolic stability in the DPPE series,[8b] into the TPE series with the hope of improving metabolic stability and maintaining or improving in vitro

potency. From this approach, we identified several advanced lead compounds such as 9d−g (Table 3). TPE fluorinated ureas 9d−g were potent having hWPA and TgWPA IC$_{50}$ values comparable to 1. In addition, these compounds showed improved metabolic stability (except for 9f) compared with the cyclopentyl analogs 9a and 9b. In Tg mouse efficacy studies, compounds 9d, 9e, and 9g exhibited complete inhibition of CETP at 10 mg/kg. Furthermore, 9d demonstrated efficacy equivalent to that of 1 at 3 mg/kg in a separate dose escalation study (AUC$_{0-8h}$ for 9d was 4.8 μM·h; AUC$_{0-8h}$

Table 4. BP Effects for TPE Ureas and Amides in Telemeterized Rats[a]

Compd #	A-ring	E	CETP hWPA IC$_{50}$ (μM)[b]	C$_{max}$ (μM)/Time point sampled	AUC$_{0-24h}$ (μM*h)	C$_{max}$ (μM)	C$_{24h}$ (μM)	BP Increase
9c	(F-phenyl)	–NH–C(=O)– aryl(F, CF$_3$)	0.62±0.30 (n=2)	9.5 / 4 hr	**270**	**9.5**	**2.5**	No effect at 30 mg/kg
9d	(CF$_3$, F-phenyl)	urea –NH–C(=O)–NH–CH$_2$CF$_3$	0.18± 0.07 (n=11)	7.3 / 2 hr	99.4	7.3	1.0	BP increase by 10-15 mmHg, 1 hr post dose, 12 hr duration at 30 mg/kg
9f	(F-phenyl)	urea –NH–C(=O)–N...–(F, F)	0.21±0.10 (n=9)	3.2 / 2 hr	28	3.2	0.2	No effect at 60 mpk
9h	(OMe, F-phenyl)	urea –NH–C(=O)–NH–CH$_2$CF$_3$	0.21±0.10 (n=9)	9.5 / 2 hr	112	9.5	1.4	No effect at 30 mg/kg
9i	(F-phenyl)	amide –NH–C(=O)–CH$_2$CH$_2$CF$_3$	0.47±0.14 (n=9)	12.3 / 6 hr	183	12.3	3.8	BP increase by 10-15 mmHg, 1 hr post dose, 12 hr duration at 60 mg/kg
9j	(CF$_3$, F-phenyl)	amide –NH–C(=O)–CH$_2$CH$_2$CF$_3$	0.43±0.14 (n=8)	12.4 / 2 hr	155	12.4	2.8	BP increase by 10-15 mmHg, 1 hr post dose, 12 hr duration at 60 mg/kg
5	(Cl-pyridine)	–NH–C(=O)– aryl(F, CF$_3$)	3.6±2.8 (n=7)	25.4 / 4 hr	**562**	**25.5**	**8.4**	No effect at 60 mg/kg
1			0.10±0.05 (n=248)	2.5 / 4 hr		2.5	0.024	BP increase by 8 mmHg, 1 hr post dose, 10 hr duration at 10 mg/kg

[a]Compound or vehicle (ethanol/cremophor/water, 1/1/8) was dosed orally to designated groups of telemeterized rats (male Sprague−Dawley, ~450 g, 17 weeks), and BP, HR, and locomotor activities were monitored for 24 h. BP, HR, and locomotor activities were recorded from 24 h prior to vehicle dosing through 24 h after dosing. Plasma exposures were assessed in two nontelemeterized satellite rats dosed with the same dosing solution. Plasma was sampled at 1, 2, 6, and 24 h after dosing in satellite rats. [b]Inhibition in the hWPA was measured in duplicate at six concentrations, and the mean values were used to calculate the IC$_{50}$. IC$_{50}$ values are reported as the mean ± SD for $n \geq 2$ (see ref 8a and Supporting Information for details).

for **1** was 2.4 μM·h); the MED for both was 3 mg/kg. Compound **9f**, on the other hand, showed a near complete inhibition of CE transfer at the 2 and 4 h time points but lost considerable activity at the 8 h time point. The reduced efficacy of **9f** over time was likely due to an increased rate of metabolism (MLM = 0.126 nmol min^{-1} mg^{-1}) resulting in lower plasma concentrations (C$_{8h}$ = 0.054 μM) in Tg mice.

Compounds in Table 3 are representative of a large set of TPE analogs, many of which demonstrated robust in vivo efficacy with complete inhibition of CE transfer activity at a 10 mg/kg oral dose in the Tg mouse studies, similar to that of compound **1**. The data in Table 3 demonstrate a strong correlation between the in vitro metabolic stability and WPA activity of a compound with its in vivo PD effects in the Tg mice (very good PK/PD correlation). Because hWPA and TgWPA data were similar across all the compounds tested and because of the excellent PK/PD relationship, we used the in vitro metabolic stability profile and hWPA potency data to guide compound selection for the Tg mouse studies.

Since a large number of CETP polymorphisms are present in the human population, some occurring at a relatively high frequency, it is important for CETP inhibitors to be comparably potent against these mutants. In the literature, compound **1** behaved similarly against a set of nine relatively common CETP variants, with no significant differences in inhibition.[22] We

therefore studied the effect of compound **9d** on CETP mutants. The studies of **9d** and **1** were carried out using the same set of nine published mutants. IC$_{50}$ inhibition values for both **9d** and **1** varied less than 3-fold across all CETP mutants tested, suggesting that the TPE derivatives as a class of CETP inhibitors were equally potent against common human CETP variants.

The moderately high-fat-, high-cholesterol-fed hamster model was our primary animal model to assess compound ability to elevate HDL-C through CETP inhibition, as the HDL/LDL profiles in this hamster model are similar to humans. The effects of compounds **9d**, **9e**, **1**, and **5** on plasma HDL-C were obtained in a 3-day study in this model. As shown in Figure 2, HDL-C was increased by all compounds. Compound **9d**, therefore, showed equivalent CETP inhibition in Tg mice and elevation of HDL-C in hamsters when compared with **1**.

Compound **1** produced a mild increase in BP in patients[6a−c] and in conscious telemeterized rats.[6d,8a,23] Therefore, the potential for compound **9d** to alter BP and heart rate (HR) was also assessed in conscious, telemeterized rats. A mild increase in mean arterial pressure (MAP) (~10−15 mmHg) lasting approximately 12 h was observed in rats treated with **9d** at 30 and 60 mg/kg single dose, po (C$_{max}$ of 14.6 and 16.3 μM, respectively), while MAP was not increased in the vehicle-

Table 5. SAR of 4-Fluoro-3-substituted Phenyl A-Ring Analogs with N-Terminus Arylamides

9c, 10a–10j
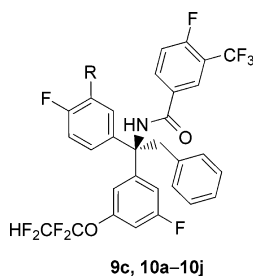
compd	R	CETP SPA IC$_{50}$ (nM)^a	CETP WPA IC$_{50}$ (μM)^a	human LM % remaining^b	mouse LM % remaining^b	po AUC$_{0-8h}$ (μM·h)^c	po C$_{8h}$ (μM)^e
9c	H	5	0.62 ± 0.30 ($n = 2$)	100	100	50.8	3.7
10a	OH	860 ± 22 ($n = 2$)	73	64	43	NT	NT
10b	OCH$_3$	7.2	0.66 ± 0.41 ($n = 2$)	100	81	21.5	1.5
10c	OCH$_2$CH$_3$	3.3	0.34 ± 0.01 ($n = 2$)	91	92	17.9	0.51
10d	OCH(CH$_3$)$_2$	4.6 ± 1.8 ($n = 8$)	0.17 ± 0.07 ($n = 23$)	82	92	9.9, 14.5^e	0.29, 0.5^e
10e	OC(CH$_3$)$_3$	2.5	0.18 ± 0.05 ($n = 2$)	92	100	3.4	0.45
10f	OCH(CH$_3$)CH$_2$OH	8	0.51	NT	NT	NT	NT
10g	O-cyclopropyl	3.8 ± 2.6 ($n = 9$)	0.22 ± 0.06 ($n = 14$)	97	100	20.4^e	1.5^e
10h	CH$_2$CH(CH$_3$)$_2$	19 ± 7 ($n = 2$)	0.92 ± 0.29 ($n = 3$)	100	76	NT	NT
10i	cyclopropyl	2.6	0.29 ± 0.05 ($n = 2$)	100	99	2.9	0.40
10j	CH$_2$N(CH$_3$)$_2$	15	0.39 ± 0.03 ($n = 2$)	null^d	null^d	1.0	0.043

^{a}Inhibition in the SPA and WPA was measured in duplicate at six concentrations, and the mean values were used to calculate the IC$_{50}$. IC$_{50}$ values are reported as the mean ± SD, for $n \geq 2$ (see ref 8a and Supporting Information for details). ^{b}Microsomal metabolic rate during 10 min incubation at 0.5 μM concentration. HLM: human liver microsomes. MLM: mouse liver microsomes. ^{c}Oral PK in Balb/c mice at 10 mg/kg, po. Vehicle: ethanol/Cremophor/water, 1/1/8. ^{d}Null: not detected. NT: not tested. ^{e}AUC$_{0-8}$ and C$_{8h}$ in Tg mouse studies (10 mg/kg, po).

treated rats. The increase in MAP for 9d was due to an elevation of both systolic and diastolic BP (SBP and DBP). Previously, TPE phenylamide 9c, a close analog to DPPE lead 5, was tested side-by-side with 5, and neither effected BP in rats (9c, C_{max} = 9.5 μM at 30 mg/kg, po; 5, C_{max} = 25.5 μM at 60 mg/kg, po), suggesting the N-terminus amides may be less at risk for BP effects than ureas.

Because of the BP increase observed with 9d, we selected a set of compounds for BP studies that showed complete CE inhibition in Tg mice at 10 mg/kg, po. Table 4 summarizes rat telemetry data for representative TPE compounds with different N-terminus groups (E) in comparison with 1 and 5. C_{max} values and time point sampled as well as plasma exposure over 24 h, determined in a satellite set of rats, are shown for each compound tested. Among linear ureas (e.g., 9d and 9h), cyclic ureas (e.g., 9f), linear amides (e.g., 9i and 9j), and arylamide N-terminus groups (e.g., 9c and 5), only arylamides consistently demonstrated no BP increase despite high and sustained exposure (AUC$_{0-24h}$ of 270 and 562 μM·h for 9c (30 mg/kg, po) and 5 (60 mg/kg, po), respectively). No effects on HR or locomotion were observed for any of the compounds tested. Thus, we turned our focus on further optimization of the arylamide series.

The phenylamides were historically less potent in the hWPA when compared with the fluorinated ureas. A breakthrough came when further modifications to the phenyl A-ring substituent were carried out. The 4-fluoro-3-methoxyphenyl A-ring in urea 9j exhibited no BP increase. In addition, its corresponding phenylamide analog 10b demonstrated hWPA activity similar to the 4-fluorophenyl A-ring analog 9c (Table 5). These findings prompted a further exploration around the substitution of the hydroxyl at the 3 position of the phenyl A-ring. As shown in Table 5, the methyl ether 10b exhibited more than a 100-fold increase in hWPA potency compared with the 3-hydroxy analog 10a. Increasing steric bulk at the 3-ether position led to an improvement in hWPA potency (methyl 10b to ethyl 10c to isopropyl 10d and tert-butyl 10e) with isopropyl ether analogs 10d and 10e being the most potent compounds in the series. Adding polar groups generally decreased hWPA potency; 10f having an isopropyl alcohol was the most potent when polar substitution was present on the A-ring. The cyclopropyl ether analog 10g was equipotent with 10d and 10e in the hWPA. The carbon linked 3-substituents, such as isopropyl 10h or cyclopropyl 10i, were also potent, as was N,N-dimethylmethylamine 10j.

It is expected that high plasma exposures and a low peak-to-trough ratio are determining factors for achieving good CETP inhibitory efficacy in vivo. In PK bridging studies, a series of compounds with high, medium, and low exposure in the Tg mouse model were tested in wild-type Balb/C mice via oral dosing. The exposures in both Tg mice and Balb/C mice were similar. Therefore, oral PK screening was performed using more cost-effective Balb/C mice with compounds having good hWPA potency and liver microsomal stability (see both AUC$_{0-8h}$ and C$_{8h}$ in Table 5). The cyclopropyl ether analog 10g stood out as having the best combination of hWPA potency and PK profile and was therefore advanced to extensive in vitro, in vivo, and liability profiling.

In Vitro, in Vivo, and Preclinical Liability Profile of Compound 10g. Compound 10g is a potent CETP inhibitor having a SPA IC$_{50}$ of 4 nM, and in the hWPA it inhibited CE transfer with an IC$_{50}$ of 0.22 μM, slightly less potent than compound 1 (IC$_{50}$ = 0.11 μM). In contrast, 10g exhibited superior potency as measured by in vivo inhibition of CE transfer when dosed orally in hCETP/apoB-100 dual Tg mice (Figure 3). Compound 10g maximally inhibited CETP activity
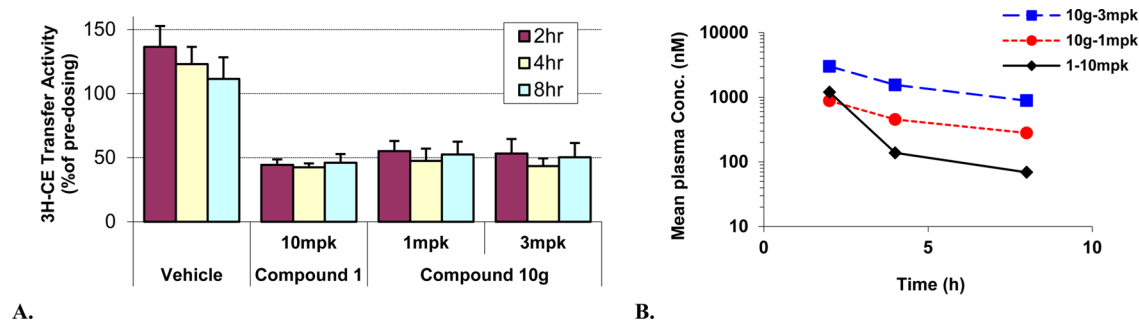
Figure 3. (A) Inhibition of plasma CE transfer activity by compound **10g** (1 and 3 mg/kg) and compound **1** (10 mg/kg) in Tg mice. (B) Exposure levels of **10g** (dose, 3 mg/kg **10g** in blue, 1 mg/kg of **10g** in red) and **1** (dose, 10 mg/kg in black), respectively, in Tg mice studies.
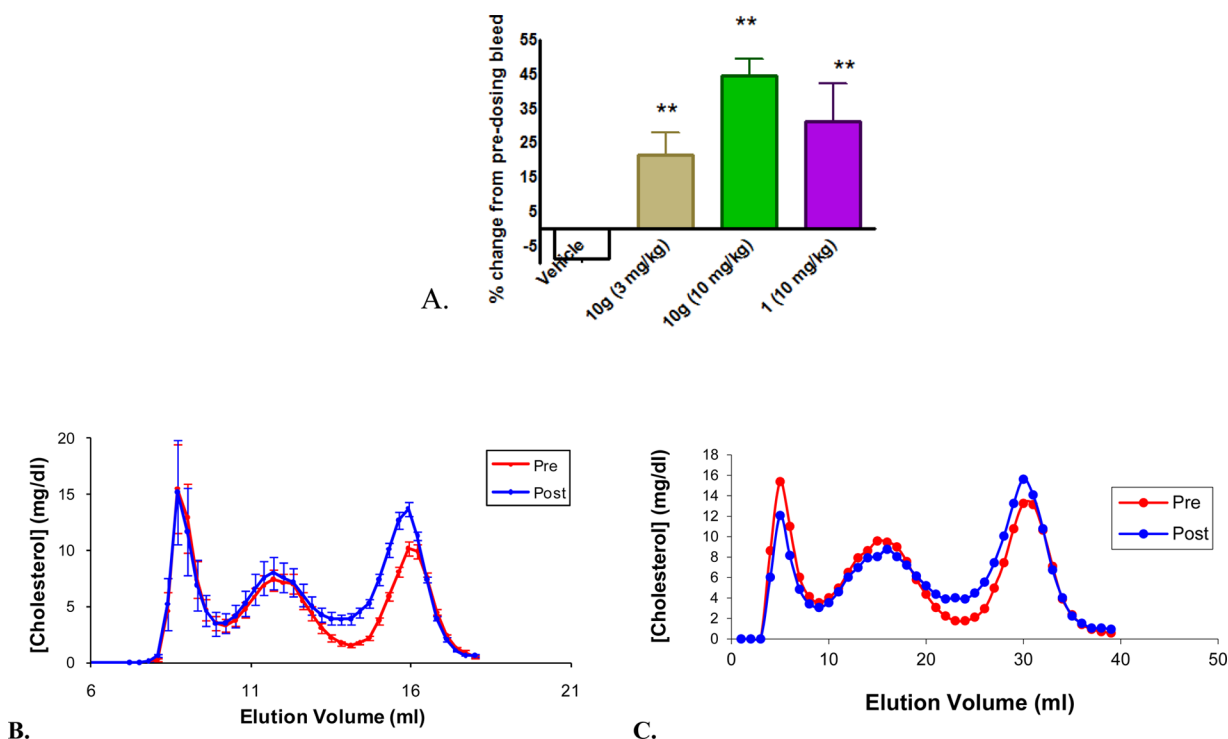
Figure 4. (A) Effect of compound **10g** (3 and 10 mg/kg, po) and compound **1** (10 mg/kg, po) on HDL-C in moderately high-fat fed hamsters dosed for 3 days (q.d.). One-way ANOVA (Dunnett's) test: (∗∗) $p < 0.01$, $n = 6$. (B) Cholesterol profiles of plasma from hamsters before and after dosing for 3 days with **10g** (10 mg/kg, po) after FPLC fractionation. (C) Cholesterol profiles of plasma from hamsters before and after dosing for 3 days with **1** (10 mg/kg, po) after FPLC fractionation.

at a dose of 1 mg/kg at the 8 h time point (Figure 3A, MED = 1 mg/kg), while in a separate study the MED for **1** was 3 mg/kg. The reason for the greater efficacy of **10g** at a lower dose is its improved plasma exposure and peak-to-trough ratio as compared with **1** (Figure 3B).

Compound **10g** increased plasma HDL-C content by 45% when dosed orally at 10 mg/kg for 3 days in moderately fat-fed hamsters (Figure 4A). The extent of HDL-C elevation was equivalent to the increase observed with **1** (51% increase in HDL-C). The plasma concentration of compound **10g** at 2 h after dosing on the third day was 4.2 μM, while the plasma concentration of compound **1** at the same time point was 1.2 μM. Plasma samples from hamsters treated with 10 mg/kg **10g** were assayed for cholesterol content after fractionation by FPLC to determine the effects of the compound on the various plasma lipoprotein classes. After each individual plasma sample was fractionated, the cholesterol content in each FPLC fraction was then averaged. By this analysis, **10g** was determined to

increase HDL-C content by 51% (Figure 4B). Plasma samples from hamsters treated with 10 mg/kg **1** were pooled before FPLC fractionation and the determination of cholesterol content (Figure 4C). The size of HDL particles was increased with **10g** to an extent similar to that observed for **1**; i.e., there was a similar leftward shift of the HDL peak in Figure 4B and Figure 4C.

The physicochemical, pharmaceutical, and pharmacokinetic properties of **10g** were analyzed to enable optimization of additional in vivo studies. Compound **10g** is an amorphous solid, and no crystalline forms were identified in a high-throughput crystallization screen. It is highly lipophilic with a calculated ACD log P of 10.4, similar to **1** and **3**. The solubility of **10g** is less than 1 μg/mL in aqueous buffer (pH 6.5) but more than 300 mg/mL in various pharmaceutically accepted nonaqueous lipids and oils. The mouse PK profile of **10g** using Cremophor/ethanol/water (10/10/80) as the vehicle for intravenous (iv) (5 mg/kg) and po (10 mg/kg) administrations

Table 6. Discrete PK Parameters of Compound 10g across Species

	mouse	rat	cyno	dog
dose (mg/kg) (route)	5 (iv)	1 (iv)	4 (iv)	1 (iv)
	10 (po)	10 (po)	5 (po)	5 (po)
formulation	Cremophor (iv)[a]	Cremophor (iv)[a]	Cremo/EtOH (iv)[b]	PEG/EtOH/H$_2$O (iv)[c]
	Miglyol (po)[d]	Gelucire (po)[e]	Gelucire (po)[e]	Miglyol (po)[d]
CL (mL min^{-1} kg^{-1})	2.0	0.9	0.9	1.4
V_{dss} (L/kg)	0.8	0.4	0.9	0.6
iv $t_{1/2}$ (h)	6	7	>18	10
iv AUC$_{0-24h}$ (μM·h)	44[f]	27	82	17
po C_{max} (μM)	5.3	17	1.7	0.43
po t_{max} (h)	1	2	5	5
po AUC$_{0-24h}$ (μM·h)	85	99	21	4
F (%)	37	37	20	5

[a]Cremophor = Cremophor/EtOH/water (10/10/80). [b]Cremo/EtOH = EtOH/Cremophor/water (12.5/2.5/85). [c]PEG/EtOH/water (70/10/20). [d]Miglyol = Miglyol 812/Capmul MCM/Triacetin/Cremophor RH40 (15/30/15/40). [e]Gelucire = Gelucire/Labrosol/Tween 80 (70/29/1). [f]AUC$_{0-8h}$.

showed low oral bioavailability (F = 7%). The low oral exposure is likely due to compound precipitation after oral administration (solubility-limited absorption). On the basis of formulation studies using the structurally similar compound **10d**, several lipid-based and spray-dried dispersion (SDD) formulations were selected and evaluated to assess the oral exposure of **10g**. Gelucire- and miglyol-based lipid formulations provided the best exposures, and compound **10g** had reasonable oral bioavailability with F values of 37%, 37%, 20%, and 5% in mice, rats, monkeys, and dogs, respectively (Table 6). Compound **10g** was not extensively distributed outside the vascular compartment in mice, rats, dogs, and monkeys. Compound **10g** was highly bound to human serum proteins (>99.6%) and serum proteins of all animal species tested (≥99.8% for rat and >99.7% for cyno). Following iv dosing, plasma concentrations of **10g** exhibited a multi-exponential decline. The total plasma clearance (CL) of **10g** after iv administration was low in mice (2.0 mL min^{-1} kg^{-1}), rats (0.9 mL min^{-1} kg^{-1}), dogs (1.4 mL min^{-1} kg^{-1}), and monkeys (0.9 mL min^{-1} kg^{-1}). This is consistent with the long half-life ($t_{1/2}$) in NADPH-fortified human liver microsomes (>86 min) and in animal liver microsomes (>94 min in mice, rats, and monkeys; 39 min in dogs). The elimination half-life ($t_{1/2}$) of **10g** after iv administration was 6, 7, >18, and 10 h in mice, rats, monkeys, and dogs, respectively. These studies supported further work with **10g** in animal studies using lipid formulations.

In telemeterized rats, compound **10g** had no effect on mean, systolic, or diastolic BP (Figure 5A), HR, or locomotor activity as compared with vehicle following iv infusion (8 mg/kg), achieving a C_{max} of 33 μM, which is a significant multiple (~30-fold) of the estimated efficacious concentration (~1 μM). In comparison, an increase in BP was seen at efficacious concentrations in rats following oral administration (C_{max} of 3.0 μM) of compound **1** (10 mg/kg) (Figure 5B).

After the termination of the ILLUMINATE trial of compound **1**, it was found that the observed increase in BP and serum electrolyte changes in humans were consistent with increasing levels of circulating aldosterone.[6d,e] In addition, **1** increased aldosterone in rats as well as aldosterone synthase in cells. The increase in aldosterone levels could be modeled in adrenocarcinoma cells (H295R) by an increase in the enzyme responsible for synthesizing aldosterone, CYP11B2 (aldosterone synthase). In studies using these cells, **1** increased
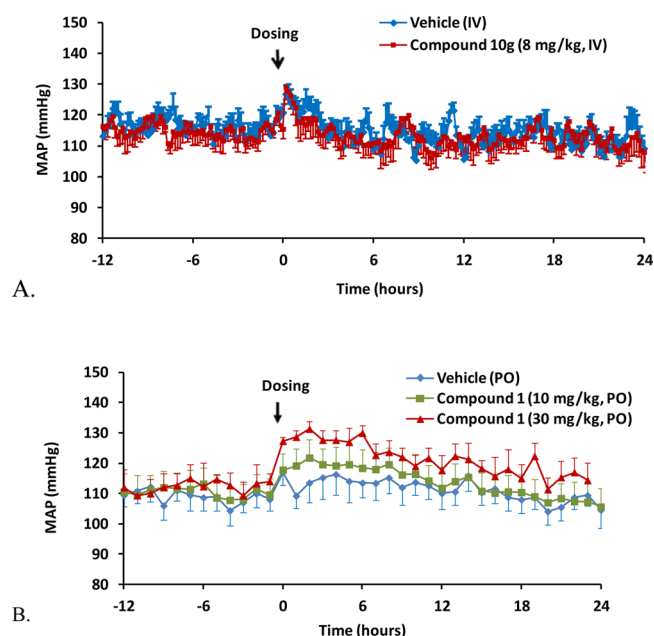
Figure 5. (A) Effect of compound **10g** on BP (8 mg/kg, iv infusion) in telemeterized rats. (B) Effect of compound **1** on BP (10 mg/kg, po, and 30 mg/kg, po, respectively) in telemeterized rats. Compound **1** increased mean arterial pressure (MAP) by 8 and 15 mmHg at 10 and 30 mg/kg (C_{max} of 3.0 and 6.5 μM), respectively. Compound or vehicle (ethanol/Cremophor/water at 1/1/8) was dosed orally to designated groups of telemeterized rats (male Sprague–Dawley, ~450 g, 17 weeks), and BP was averaged over either a 10 min or 1 h time frame. Each data point is expressed as the mean ± SEM. Data were compared between compound and vehicle group using repeated ANOVA with Dunnett's post hoc test.

CYP11B2 mRNA at a concentration as low as 3 nM and by up to 90-fold at 300 nM. In contrast, compound **10g** did not increase CYP11B2 mRNA at 10 μM (Figure 6).

Overall, compound **10g**, being structurally different from the four clinical compounds **1**−**4**, demonstrated favorable in vitro and in vivo properties and a lack of off-target effects on BP and aldosterone levels in cells compared to **1**. Therefore, **10g** was selected for preclinical safety studies.
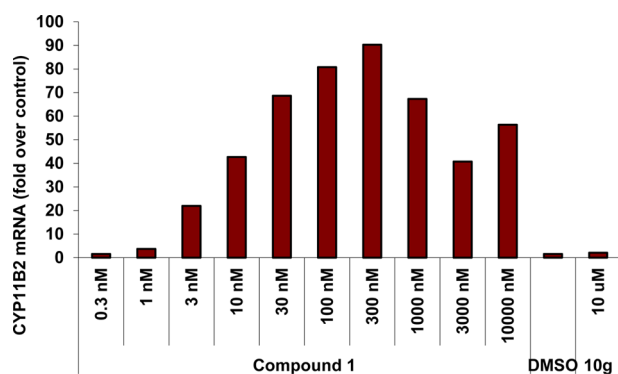
Figure 6. Effects of compound **1** and **10g** on CYP11B2 expression in H295R cells. Compounds were incubated with the cells at the indicated concentrations for 24 h, and CYP11B2 mRNA levels were measured and compared to the levels in vehicle (DMSO)-treated cells.

CONCLUSIONS

Lead optimization efforts on the DPPE pyridyl A-ring led to the discovery of a series of TPE ureas and amides with improved in vitro hWPA potency and in vivo inhibition of CE transfer in Tg mice as compared with the DPPE lead **5**. Subsequent screening of compound effects on BP in telemeterized rats allowed us to focus on the modification of the 3,4-disubstituted phenyl A-rings in the amide series, resulting in the discovery of TPE amide **10g**. Compound **10g** is a potent CETP inhibitor having a preclinical liability profile superior to the benchmark CETP inhibitor, compound **1**. Compound **10g** demonstrated dose-dependent CETP inhibition in Tg mice with a MED of 1 mg/ kg and a comparable increase in HDL-C content and size in hamsters as compared with **1**. In contrast to the off-target BP and aldosterone synthase (CYP11B2) increases observed with **1**, compound **10g** did not increase BP in rat telemetry studies and did not increase aldosterone synthase (CYP11B2) in vitro. As a result, compound **10g** was selected for preclinical safety studies.

EXPERIMENTAL SECTION

General Information. All reagents and solvents used, including anhydrous solvents, were of commercial quality. All reactions were carried out under a static atmosphere of argon or nitrogen and stirred magnetically unless otherwise stated. All flash chromatographic separations were performed using either an ISCO RediSep disposable silica gel column or a biotage column, eluting with hexanes/ethyl acetate or methylene chloride/methanol. For large amount of diastereomeric mixtures, the desired compound was obtained via SFC on the Thar 350 system. The SFC conditions were 20% isopropanol in CO_2 at 240 mL/min on Chiralpak AD-H (5 cm × 25 cm); wavelength, 254 nm; back pressure, 100 bar; sample concentration, 110 mg/mL; injection volume, 10 mL; cycle time, 6.5 min; temperature, 35 °C. Final compounds were also purified by reverse phase HPLC on a Sunfire C18 preparative column using appropriate gradients of acetonitrile/water/0.1% trifluoroacetic acid or methanol/water/0.1% trifluoroacetic acid as the eluent. Reactions were monitored either by analytical LCMS or by TLC using 0.25 mm E. Merck silica gel plates (60 F_{254}) and were visualized with UV light or by staining with various of staining agents. LCMS data were recorded on a Shimadzu LC-10AT equipped with a SIL-10A injector, a SPD-10AV detector, running DISCOVERY VP software, and coupled with a Waters ZQ mass spectrometer running MassLynx, version 3.5, software using the following methods: Phenomenex Luna C-18 4.6 mm × 50 mm column eluted with a 4 min linear gradient from 0% to 100% of B and then 1 min at 100% of B wherein A = 10% methanol/ 90% water/0.1% TFA and B = 90% methanol/10% water/0.1% TFA

(method A). Phenomenex Luna C-18 2.0 mm × 30 mm column eluted with a 2 min linear gradient from 0% to 100% of B and then 1 min at 100% of B wherein A = 10% methanol/90% water/0.1% TFA and B = 90% methanol/10% water/0.1% TFA (method B). Phenomenex Luna C-18 2.0 mm × 30 mm column eluted with a 2 min linear gradient from 0% to 100% of B and then 1 min at 100% of B wherein A = 2% methanol/98% water/0.1% formic acid and B = 100% methanol/0.1% formic acid (method C). Phenomenex Luna C-18 4.6 mm × 50 mm column eluted with a 4 min linear gradient from 10% to 100% of B and then 1 min at 100% of B wherein A = 10% methanol/90% water/0.1% NH_4OAc and B = 90% methanol/10% water/0.1% NH_4OAc (method D). Purity of all final compounds tested was determined to be at or above 95% by using the following orthogonal HPLC conditions: Sunfire C18 3.5 μm (3.0 mm × 150 mm), flow rate 1.0 mL/min, gradient 10−100% 95:5 AcCN in H_2O (0.05% TFA) in 5:95 AcCN in H_2O (0.05% TFA) over 10 min and then 100% of 95:5 AcCN in H_2O (0.05% TFA) over 5 min (HPLC method A) and Xbridge phenyl 3.5 μm (3.0 mm × 150 mm), flow rate 1.0 mL/min, gradient 10−100% 95:5 AcCN in H_2O (0.05% TFA) in 5:95 AcCN in H_2O (0.05% TFA) over 10 min and then 100% of 95:5 AcCN in H_2O (0.05% TFA) over 5 min (HPLC method B) or Sunfire, 150 mm × 4.6 mm, 3 mm, flow rate 1.0 mL/min, gradient 65−95% gradient AcCN in H_2O (0.05% TFA) over 30 min and then 95% of AcCN in H_2O (0.05% TFA) over 5 min (HPLC method C) or Zorbax SB-C8 3.5 μm, 150 mm (L) × 4.6 mm, flow rate 1.0 mL/min, gradient 55−95% AcCN in H_2O (0.05% TFA) over 30 min and then 95% of AcCN in H_2O (0.05% TFA) over 5 min (HPLC method D) and/or elemental analyses. ^{1}H NMR, ^{13}C NMR, or ^{19}F NMR spectra were recorded on either Bruker or JEOL Fourier transform spectrometers operating at frequencies as follows: ^{1}H NMR, 400 MHz (Bruker or JEOL) or 500 MHz (JEOL); ^{13}C NMR, 101 MHz (Bruker or JEOL) or 125 MHz (JEOL); and ^{19}F NMR, 471 MHz (Bruker or JEOL). Spectra data are reported in the format chemical shift (multiplicity, coupling constants, and number of hydrogens). Chemical shifts are specified in ppm referenced to deuterated solvent peaks. All ^{13}C NMR and ^{19}F NMR spectra were proton decoupled. Most of the final compounds were confirmed for molecular weight using accurate mass LCMS (HRMS). A Thermo Fisher LTQ Orbitrap mass spectrometer in line with a Waters Acquity UPLC allowed collection of molecular ion data with accuracy of <5 ppm.

3-Cyclopentyl-1-[(1*R***)-1-[4-fluoro-3-(trifluoromethyl)-phenyl]-1-[3-fluoro-5-(trifluoromethyl)phenyl]-2-phenylethyl]-urea (8b) and 3-Cyclopentyl-1-[(1***S***)-1-[4-fluoro-3-(trifluoromethyl)phenyl]-1-[3-fluoro-5-(trifluoromethyl)-phenyl]-2-phenylethyl]urea (8c).** An ether solution (40 mL) of 1-bromo-3-fluoro-5-(trifluoromethyl)benzene (2.00 g, 8.23 mmol) was stirred in an oven-dried round-bottom flask at −78 °C under Ar. *n*-BuLi (2.5 M in hexanes, 3.6 mL, 9.1 mmol, 1.1 equiv) was added dropwise. The resulting solution was stirred at −78 °C for 30 min. A solution of 4-fluoro-3-(trifluoromethyl)benzonitrile (1.55 g, 8.23 mmol, 1.0 equiv) in Et_2O (5 mL) was added dropwise. The resulting reddish mixture was stirred at −78 °C for 2 h. TMSCl (pretreated with Et_3N, TMSCl/Et_3N = 10:1 (v:v), 1.1 mL, 1.2 equiv) was added dropwise. The dry ice bath was removed, and the resulting slurry was stirred at room temperature for 2 h. The reaction was cooled to −78 °C, and a solution of benzylmagnesium chloride in THF (2.0 M, 8.4 mL, 2.0 equiv) was added dropwise. The resulting mixture was slowly warmed up to room temperature and stirred at room temperature for 16 h. The reaction flask was cooled in an ice bath, and 1 N HCl (100 mL) was added. The mixture was stirred at room temperature for 30 min, extracted with Et_2O (2×), washed with 1 N NaOH, H_2O, and brine, dried over Na_2SO_4, filtered, and concentrated to dryness. The residue was purified by flash column chromatography (silica gel, hexanes:ethyl acetate) to give 1-[4-fluoro-3-(trifluoromethyl)phenyl]-1-[3-fluoro-5-(trifluoromethyl)phenyl]-2-phenylethan-1-amine (**13b**) (1.6 g, 44%). LCMS ESI 429.2 [M − NH_3 + H]$^+$, t_R = 3.42 min (method A). ^{1}H NMR (400 MHz, CDCl$_3$) δ ppm 7.66 (dd, *J* = 6.7, 2.3 Hz, 1H), 7.49−7.59 (m, 1H), 7.45 (s, 1H), 7.18−7.30 (m, 6H), 6.74 (d, *J* = 6.9 Hz, 2H), 3.57 (m, 2H). ^{13}C NMR (101 MHz, MeOD) δ ppm 163.74 (d, *J* = 249.0 Hz), 159.94 (dq, *J* = 255.7, 3.0 Hz), 153.24

(d, *J* = 6.8 Hz), 144.91 (d, *J* = 3.8 Hz), 136.68, 134.53 (d, *J* = 9.1 Hz), 133.35 (qd, *J* = 33.1, 8.2 Hz), 132.01, 129.07, 128.05, 126.92 (q, *J* = 4.5 Hz), 124.84 (qd, *J* = 272.5, 3.2 Hz), 124.16 (q, *J* = 271.6 Hz), 121.01 (m), 119.31 (d, *J* = 23.0 Hz), 118.73 (qd, *J* = 32.7, 12.7 Hz), 117.85 (d, *J* = 20.6 Hz), 112.16 (dq, *J* = 24.7, 3.5 Hz), 62.54, 48.87. ^{19}F NMR (471 MHz, MeOD) δ ppm −62.61 (d, *J* = 16.2 Hz), −64.05, −111.96, −119.13 (q, *J* = 12.8 Hz). Compound **13b** (300 mg, 0.67 mmol) and cyclopentyl isocyanate (0.4 mL, 3.9 mmol, 5.8 equiv) were stirred in 1,4-dioxane (2 mL) at room temperature for 16 h. The reaction mixture was concentrated and purified by flash chromatography (silica gel, hexanes/EtOAc) to give **14b** (250 mg, 67%). The racemate **14b** (250 mg) was dissolved in 10% isopropanol in heptane and was resolved by chiral prep HPLC using an AD column (10% isopropanol/heptane/0.1% DEA, isocratic) to give the fast eluting enantiomer corresponding to **8c** (110 mg, 44%); analytical chiral HPLC (AD column, 10% isopropanol/heptane/0.1% DEA, isocratic), 99%, t_R = 4.85 min; and the slow eluting enantiomer corresponding to **8b** (105 mg, 42%): analytical chiral HPLC (AD, 10% isopropanol/heptane/0.1% DEA, isocratic), 99%, t_R = 14.11 min. LCMS (ESI), 557.32 [M + H]$^+$, t_R = 4.33 min (method A). ^{1}H NMR (400 MHz, CDCl$_3$) δ ppm 7.36−7.44 (m, 2H), 7.23−7.29 (m, 3H), 7.13−7.21 (m, 4H), 6.68−6.74 (m, 2H), 4.84 (s, 1H), 4.40 (s, br, 1H), 3.84−3.95 (m, 3H), 1.88−1.98 (m, 2H), 1.56−1.68 (m, 4H), 1.34 (d, *J* = 6.36 Hz, 2H). ^{13}C NMR (101 MHz, MeOD) δ 163.86 (d, *J* = 247.5 Hz), 160.37 (dd, *J* = 255.8, 2.0 Hz), 159.36 (d, *J* = 2.1 Hz), 151.71 (d, *J* = 6.8 Hz), 143.15 (m), 137.26, 134.58 (d, *J* = 9.0 Hz), 133.21 (qd, *J* = 33.1, 8.3 Hz), 132.10, 128.80, 127.91, 126.72 (q, *J* = 4.6 Hz), 124.84 (dq, *J* = 271.6, 2.9 Hz), 124.10 (q, *J* = 271.2 Hz), 120.83 (m), 119.31 (d, *J* = 23.4 Hz), 118.46 (qd, *J* = 32.4, 12.8 Hz), 117.82 (d, *J* = 21.2 Hz), 112.18 (dq, *J* = 25.3, 3.7 Hz), 63.39, 63.32, 52.73, 44.96, 34.35, 24.48. ^{19}F NMR (471 MHz, MeOD) δ −62.85 (d, *J* = 12.7 Hz), −64.22, −112.35, −119.42 (q, *J* = 12.9 Hz). Orthogonal HPLC purity: 96.5%, t_R = 14.25 min (HPLC method A); 95.6%, t_R = 10.91 min (HPLC method B).

4-Fluoro-*N*-[(1*R*)-1-[3-fluoro-5-(1,1,2,2-tetrafluoroethoxy)phenyl]-1-(4-fluorophenyl)-2-phenylethyl]-3-(trifluoromethyl)-benzamide (9c). To a solution of **18** (30 mg, 0.079 mmol) in CH$_2$Cl$_2$ (0.2 mL) was added 4-fluoro-3-(trifluoromethyl)benzoyl chloride (0.048 mL, 0.16 mmol), followed by Et$_3$N (0.040 mL, 0.16 mmol). The resulting mixture was stirred at room temperature for 5 h. The crude product was purified on a preparative C18 HPLC column using 30−100% CH$_3$CN in H$_2$O with 0.1% TFA as the mobile phase. The solvent was removed under reduced pressure to afford **9c** (43 mg, 95%) as a white powder. LCMS (ESI) *m/z* 568.30 [M + H]$^+$, t_R = 4.27 min (method A). ^{1}H NMR (400 MHz, MeOD) δ ppm 8.10−7.78 (m, 2H), 7.44 (t, *J* = 9.4 Hz, 1H), 7.28−6.87 (m, 10H), 6.71 (d, *J* = 7.0 Hz, 2H), 6.28 (tt, *J* = 52.7, 3.0 Hz, 1H), 4.10 and 3.92 (ABq, *J* = 12.7 Hz, 2H). ^{13}C NMR (101 MHz, CDCl$_3$) δ 164.35, 162.58 (d, *J* = 249.5 Hz), 162.02 (d, *J* = 248.8 Hz), 161.78 (d, *J* = 262.5 Hz), 149.35 (d, *J* = 11.5 Hz), 148.32 (d, *J* = 8.1 Hz), 138.37 (d, *J* = 3.0 Hz), 134.98, 132.54 (d, *J* = 9.6 Hz), 131.20 (d, *J* = 4.1 Hz), 130.66, 128.71 (d, *J* = 8.0 Hz), 128.28, 127.52, 126.49 (m), 122.00 (q, *J* = 272.4 Hz), 119.12 (m), 117.60 (d, *J* = 21.8 Hz), 116.44 (tt, *J* = 273.5, 29.1 Hz), 116.36 (d, *J* = 3.3 Hz), 115.43 (d, *J* = 21.1 Hz), 112.85 (d, *J* = 23.6 Hz), 108.50 (d, *J* = 24.6 Hz), 107.48 (tt, *J* = 252.9 41.0 Hz), 64.92, 44.86. ^{19}F NMR (471 MHz, MeOD) δ ppm −61.71 (d, *J* = 12.7 Hz), −88.40 (m), −108.70 (m), −109.09 (t, *J* = 9.5 Hz), −114.05 (m), −137.81 (m). Orthogonal HPLC purity: 100%, t_R = 14.30 min (HPLC method A); 97.7%, t_R = 11.34 min (HPLC method B). HRMS (M + H)$^+$ ESI calcd for C$_{30}$H$_{20}$F$_{10}$NO$_2$ 616.13283, found 616.13338.

1-[(1*R*)-1-[4-Fluoro-3-(trifluoromethyl)phenyl]-1-[3-fluoro-5-(1,1,2,2-tetrafluoroethoxy)phenyl]-2-phenylethyl]-3-(2,2,2-trifluoroethyl)urea (9d). To a solution of **24** (85 mg, 0.11 mmol) in THF (1.5 mL) was added TBAF (1.0 M in THF, 0.12 mL, 0.12 mmol) at 0 °C. The mixture was stirred at 0 °C to room temperature for 50 min. The reaction was diluted with CH$_2$Cl$_2$, washed with saturated NH$_4$Cl, H$_2$O, and then saturated NaCl, dried over Na$_2$SO$_4$, filtered, and concentrated. The residue was purified by flash chromatography (silica gel, hexanes/EtOAc) to give 1-[(1*R*)-1-[4-fluoro-3-(trifluoromethyl)phenyl]-1-(3-fluoro-5-hydroxyphenyl)-2-

phenylethyl]-3-(2,2,2-trifluoroethyl)urea (45 mg, 77%). LCMS (ESI) *m/z* 519.10 [M + H]$^+$, t_R = 2.0 min (method B). ^{1}H NMR (400 MHz, CDCl$_3$) δ ppm 7.20−7.27 (m, 3H), 7.09−7.18 (m, 3H), 6.72 (d, *J* = 9.60 Hz, 1H), 6.66 (m, 3H), 6.57 (s, 1H), 3.73−3.78 (m, 1H), 3.65−3.71 (m, 1H), 3.63 (d, *J* = 8.59 Hz, 1H), 3.47−3.58 (m, 1H). To a solution of the above phenol (15 mg, 0.03 mmol) in DMSO (0.1 mL) were added ICF$_2$CF$_2$H (11 mg, 0.05 mmol) and K$_2$CO$_3$ (20 mg, 0.14 mmol). The reaction mixture was heated in a capped vial at 70 °C for 16 h. After cooling to rt, it was purified by flash chromatography (silica gel, hexanes/EtOAc) to give compound **9d** as a white solid (18 mg, 58%). LCMS (ESI) *m/z* 619.2 [M + H]$^+$, t_R = 4.09 min (method A). ^{1}H NMR (400 MHz, MeOD) δ ppm 7.52−7.43 (m, 1H), 7.39 (dd, *J* = 6.0, 2.2 Hz, 1H), 7.26 (t, *J* = 9.6 Hz, 1H), 7.21−7.07 (m, 3H), 7.05−6.91 (m, 3H), 6.72 (d, *J* = 7.1 Hz, 2H), 6.28 (tt, *J* = 52.2, 3.0 Hz, 1H), 3.95 and 3.83 (ABq, *J* = 12.8 Hz, 2H), 3.88−3.71 (m, 1H). ^{13}C NMR (101 MHz, MeOD) δ ppm 162.63 (d, *J* = 249.0 Hz), 158.74 (d, *J* = 259.6 Hz), 155.48, 149.43 (d, *J* = 11.7 Hz), 148.13 (d, *J* = 9.0 Hz), 140.39 (d, *J* = 3.7 Hz), 134.77, 132.48 (d, *J* = 8.3 Hz), 130.71, 128.17, 127.37, 125.35 (m), 124.24 (q, *J* = 279.4 Hz), 122.36 (q, *J* = 275.5 Hz), 118.12 (qd, *J* = 33.0, 12.8 Hz), 116.99 (d, *J* = 20.8 Hz), 116.40 (tt, *J* = 273.5, 29.0 Hz), 115.96 (d, *J* = 2.6 Hz), 112.46 (d, *J* = 23.3 Hz), 108.66 (d, *J* = 24.5 Hz), 107.44 (tt, *J* = 252.0, 41.8 Hz), 64.13, 44.49, 41.39 (q, *J* = 34.4 Hz). ^{19}F NMR (471 MHz, CDCl$_3$ + MeOD) δ ppm −61.57 (d, *J* = 13.9 Hz), −73.63, −88.58, −109.43, −117.71 (q, *J* = 13.5 Hz), −137.05 (t, *J* = 6.0 Hz). Orthogonal HPLC purity: 99.5%, t_R = 13.34 min (HPLC method A); 97.6%, t_R = 10.58 min (HPLC method B). Chriral analytical HPLC (AD, 20% heptane/IPA/0.1% DEA), t_R = 8.91 min, chiral purity >99%. HRMS (M + H)$^+$ ESI calcd for C$_{26}$H$_{19}$F$_{12}$N$_2$O$_2$ 619.12495; found, 619.12517.

4-Fluoro-*N*-[(1*R*)-1-(4-fluoro-3-hydroxyphenyl)-1-[3-fluoro-5-(1,1,2,2-tetrafluoroethoxy)phenyl]-2-phenylethyl]-3-(trifluoromethyl)benzamide (10a). To a solution of **10b** (2.8 g, 4.43 mmol), prepared according to procedures described for the synthesis of compound **9c**, in CH$_2$Cl$_2$ (15 mL) was added BBr$_3$ (12 mL, 12 mmol). The resulting mixture was stirred at room temperature for 2 h and quenched by addition of ice. The reaction mixture was diluted with EtOAc and washed with saturated NaHCO$_3$, saturated NaCl, dried over Na$_2$SO$_4$, filtered, and concentrated to afford **10a** as a slightly yellow solid (2.9 g, 100%). LCMS (ESI) *m/z* 632.2 [M + H]$^+$, t_R = 4.23 min (method A). ^{1}H NMR (300 MHz, CDCl$_3$) δ ppm 7.90−7.76 (m, 2H). 7.23−7.11 (m, 4H), 7.04−6.88 (m, 4H), 6.81−6.56 (m, 5H), 5.84 (tt, *J* = 52.7, 2.9 Hz, 1H), 5.27 (s, 1H), 3.95 (d, *J* = 13.2 Hz, 1H), 3.79 (d, *J* = 13.2 Hz, 1H). ^{13}C NMR (101 MHz, CDCl$_3$) δ ppm 164.86, 162.48 (d, *J* = 249.5 Hz), 161.74 (d, *J* = 261.9 Hz), 150.28 (d, *J* = 241.5 Hz), 149.24 (d, *J* = 12.7 Hz), 148.08 (d, *J* = 7.5 Hz), 143.61 (d, *J* = 15.3 Hz), 139.42 (d, *J* = 5.3 Hz), 134.96, 132.53 (d, *J* = 10.2 Hz), 131.01, 130.58, 128.18, 127.45, 126.48, 122.95 (q, *J* = 272.4 Hz), 119.17 (m), 118.83 (d, *J* = 7.2 Hz), 117.55 (d, *J* = 20.5 Hz), 116.37 (tt, *J* = 272.0, 29.0 Hz), 116.27 (d, *J* = 34.3 Hz), 115.45 (d, *J* = 20.4 Hz), 112.64 (d, *J* = 22.9 Hz), 108.35 (d, *J* = 25.5 Hz), 107.41 (tt, *J* = 251.1, 41.2 Hz), 64.91, 44.11. ^{19}F NMR (471 MHz, CDCl$_3$) δ ppm −61.62 (d, *J* = 11.5 Hz), −88.34, −108.45, −108.99 (m), −136.68 (d, *J* = 52.5 Hz), −140.04. HRMS (M + H)$^+$ ESI calcd for C$_{30}$H$_{20}$F$_{10}$NO$_3$ 632.12776, found 632.12876. Orthogonal HPLC purity: 99.7%, t_R = 12.27 min (HPLC method A); 99.3%, t_R = 10.63 min (HPLC method B).

4-Fluoro-*N*-[(1*R*)-1-[4-fluoro-3-(propan-2-yloxy)phenyl]-1-[3-fluoro-5-(1,1,2,2-tetrafluoroethoxy)phenyl]-2-phenylethyl]-3-(trifluoromethyl)benzamide (10d). To a solution of **10a** (2.70 g, 4.27 mmol) in DMF (6 mL) was added K$_2$CO$_3$ (1.47 g, 10.69 mmol), followed by isopropyl iodide (0.64 mL, 6.40 mmol). The reaction mixture was stirred at 60 °C for 16 h. The reaction mixture was filtered, and the solid was washed with EtOAc. The filtrate was washed with H$_2$O, saturated NaCl, dried over Na$_2$SO$_4$, and concentrated under reduced pressure. The residue was purified by ISCO silica gel column using 0−50% EtOAc in hexane as eluting solvents to yield **10d** as an off-white solid (2.4 g, 83% yield). LCMS (ESI) *m/z* 674.1 [M + H]$^+$, t_R = 4.05 min (method A). ^{1}H NMR (500 MHz, MeOD) δ ppm 8.01−7.95 (m, 2H), 7.44 (dd, *J* = 10.2, 8.5 Hz, 1H), 7.21−7.16 (m, 1H), 7.15−7.09 (m, 3H), 7.06 (s, 1H), 7.03 (dd, *J* = 8.2 Hz, 1H), 6.99 (dt, *J*

= 8.8, 2.2 Hz, 1H) 6.80 (dd, J = 8.0 Hz, 1H), 6.78−6.74 (m, 1H), 6.73 (d, J = 7.1 Hz, 2H), 6.27 (tt, J = 52.5, 3.0 Hz, 1H), 4.29 (q, J = 6.0 Hz, 1H), 4.12 and 3.85 (ABq, J = 13.2 Hz, 2H), 1.23 (d, J = 6.0 Hz, 3H), 1.17 (d, J = 6.0 Hz, 3H). ^{13}C NMR (101 MHz, MeOD) δ ppm 168.45. 163.78 (d, J = 246.4 Hz), 162.84 (dq, J = 259.9, 2.3 Hz), 154.00 (d, J = 245.7 Hz), 150.85 (d, J = 8.4 Hz), 150.51 (d, J = 11.4 Hz), 146.33 (d, J = 11.4 Hz), 140.97 (d, J = 3.1 Hz), 137.40, 135.29 (d, J = 9.2 Hz), 133.58 (d, J = 3.8 Hz), 132.03, 128.83, 128.08 (qd, J = 4.6, 2.3 Hz), 127.98, 123.74 (q, J = 271.6 Hz), 121.37 (d, J = 6.9 Hz), 119.26 (qd, J = 33.6, 13.4 Hz), 118.53 (d, J = 1.5 Hz), 118.52 (d, J = 21.4 Hz), 118.16 (d, J = 2.3 Hz), 117.98 (tt, J = 271.6, 29.0 Hz), 116.51 (d, J = 19.1 Hz), 114.23 (d, J = 23.7 Hz), 109.32 (tt, J = 249.5, 40.4 Hz), 109.09 (d, J = 25.9 Hz), 73.37, 66.79 (d, J = 1.5 Hz), 44.08, 22.28, 22.19. ^{19}F NMR (376 MHz, MeOD) δ ppm −139.79 (dd, J = 6.8, 4.6 Hz, 2F), −137.20 (s, 1F), −112.74 to −112.55 (m, 2F), −90.65 to −90.51 (m, 2F), −63.57 (d, J = 11.4 Hz, 3F). HRMS (M − H)$^−$ ESI calcd for C$_{33}$H$_{24}$F$_{10}$NO$_3$ 672.1602, found 672.1595. Purity by HPLC/UV with detection at 220 nm: >99.9%, t_R = 19.23 min (HPLC method C). Analytical chiral HPLC (Chiralpak AD-H, 150 mm × 4.6 mm, 5 μm, 5% isopropanol/heptane/0.1% DEA, isocratic, 20 min), >99.9%, t_R = 10.39 min. Anal. Calcd for C$_{33}$H$_{25}$F$_{10}$NO$_3$: C, 58.84; H, 3.74; N, 2.08; F: 28.20. Found: 58.88; H, 3.71; N, 2.02; F: 28.16. Specific rotation at 589 nm: [α]$_D^{25}$ +9.549 (c 1.03, MeOH).

(N-[(1R)-1-(3-Cyclopropoxy-4-fluorophenyl)-1-[3-fluoro-5-(1,1,2,2-tetrafluoroethoxy)phenyl]-2-phenylethyl]-4-fluoro-3-(trifluoromethyl)benzamide (10g). To a 3 L, flame-dried, four-necked round-bottom flask equipped with a thermometer, a mechanical stirrer, an additional funnel, and a N$_2$ inlet were charged 1 N Et$_2$Zn in hexane (422.1 mL, 422.1 mmol), and dry CH$_2$Cl$_2$ (500 mL) under N$_2$. The solution was cooled to −10 °C. Trifluoroacetic acid (32.5 mL, 422.1 mmol) was added dropwise over a period of 1 h at below 0 °C. After 10 min, diiodomethane (34.1 mL, 422.1 mmol) was added at 0 °C. After the mixture was stirred for 15 min at 0 °C, a solution of **27** (92.5 g, 141 mmol) in CH$_2$Cl$_2$ (600 mL) was added portionwise. The reaction mixture was then allowed to warm to rt over a period of 21 h. 1 N HCl (1 L) was added, and the mixture was stirred for 15 min. The organic phase was separated, and the aqueous layer was extracted with CH$_2$Cl$_2$ (1 L). The combined organic phases were washed with brine (1.5 L) and then concentrated in vacuo. The residue yellow oil (120 g) was dissolved in CH$_2$Cl$_2$ (150 mL). The solution was subjected to a flash column packed with 1.5 kg of silica gel in hexane. The column was then eluted with CH$_2$Cl$_2$ in hexane (20−50%) to give BMS-795311 (**10g**) (91.0 g, 96%) as a white solid, after high vacuum drying for 20 h. ^{1}H NMR (400 MHz, MeOD) δ ppm 8.02−7.95 (m, 2H). 7.44 (t, J = 9.8 Hz, 1H), 7.23−7.16 (m, 2H), 7.16−7.10 (m, 3H), 7.07 (dd, J = 8.0, 2.4 Hz, 1H), 7.04−6.96 (m, 1H), 6.99 (d, J = 11.0 Hz, 1H), 6.73 (d, J = 7.1 Hz, 2H), 6.69 (ddd, J = 8.7, 3.8, 2.6 Hz, 1H), 6.27 (tt, J = 52.5, 3.1, 2.9 Hz, 1H), 4.22 and 3.77 (ABq, J = 13.0 Hz, 2H), 3.59−3.51 (m, 1H), 0.73−0.49 (m, 4H). ^{13}C NMR (101 MHz, MeOD) δ ppm 168.44, 163.83 (d, J = 246.4 Hz), 162.86 (dd, J = 260.2, 1.5 Hz), 152.60 (d, J = 245.7 Hz), 150.97 (d, J = 7.6 Hz), 150.56 (d, J = 11.4 Hz), 147.34 (d, J = 10.7 Hz), 140.74 (d, J = 3.8 Hz), 137.43, 135.30 (d, J = 9.9 Hz), 133.61 (d, J = 3.8 Hz), 132.12, 128.83, 128.03−128.15 (m), 128.01, 123.74 (q, J = 271.6 Hz), 119.26 (m), 118.56 (d, J = 21.4 Hz), 118.21 (d, J = 3.1 Hz), 116.46 (d, J = 1.5 Hz), 116.23 (d, J = 18.3 Hz), 118.00 (tt, J = 272.0, 29.0 Hz), 114.29 (d, J = 23.7 Hz), 109.11 (d, J = 25.2 Hz), 109.33 (tt, J = 249.9, 40.4 Hz), 66.85 (m), 52.39, 44.15, 6.49. ^{19}F NMR (471 MHz, MeOD) δ ppm −139.20 (d, J = 51.8 Hz, 2F), − 138.45 (br s, 1F), −112.04 (m, 2F), −90.01 (br s, 2F), −62.98 (m, 3F). HRMS (M − H)$^−$ ESI calcd for C$_{33}$H$_{22}$F$_{10}$NO$_3$ 670.14455, found 670.14335. Purity by HPLC/UV with detection at 220 nm: >99.9%, t_R = 10.59 min (HPLC method D). Analytical chiral HPLC (RR-Whelk-01, 250 mm × 4.6 mm, 10 μm, 20% isopropanol/heptane/0.1% DEA, isocratic, 20 min), >99.9%, t_R = 11.29 min. Anal. Calcd for C$_{33}$H$_{23}$F$_{10}$NO$_3$: C, 59.02; H, 3.45; N, 2..09; F, 28.72. Found: 58.95; H, 3.38; N, 1.96; F, 26.71. Specific rotation at 589 nm: [α]$_D^{25}$ +18.02 (c 0.93, MeOH).

(R)-N-[(1Z/E)-[3-Fluoro-5-(1,1,2,2-tetrafluoroethoxy)phenyl]-(4-fluorophenyl)methylidene]-2-methylpropane-2-sulfinamide (16). To an oven-dried round-bottomed flask cooled at −78 °C was

added 1-bromo-3-fluoro-5-(1,1,2,2-tetrafluoroethoxy)benzene (7.20 g, 24.8 mmol) in anhydrous ether (300 mL) under argon, and the mixture was stirred at −78 °C for 10 min. n-BuLi (2.5 M in hexanes, 11.5 mL, 28.8 mmol, 1.16 equiv) was added dropwise at −78 °C. The reaction mixture was stirred at −78 °C for 45 min. An Et$_2$O solution (20 mL) of 4-fluorobenzonitrile (3.06 g, 25.3 mmol, 1.02 equiv) was added dropwise. The resulting reddish solution was stirred at −78 °C for 2 h. The reaction mixture was quenched by adding 1 N HCl (200 mL), and the dry ice−acetone bath was removed. The resulting slurry was stirred at room temperature for 1 h followed by the addition of Et$_2$O (100 mL). The organic layer was separated and then washed with saturated NaHCO$_3$, H$_2$O, brine, dried over MgSO$_4$, filtered, and concentrated to dryness. The residue was purified by flash chromatography (EtOAc/hexanes = 0−30%) to give (3-fluoro-5-(1,1,2,2-tetrafluoroethoxy)phenyl)(4-fluorophenyl)methanone as a slightly tan oil (7.2 g, 87%). LCMS (ESI) m/z 335.31 [M + H]$^+$, t_R = 3.81 min (method A). ^{1}H NMR (500 MHz, CDCl$_3$) δ ppm 7.91−7.72 (m, 2H), 7.55−7.35 (m, 2H), 7.25−7.09 (m, 3H), 5.92 (tt, J = 52, 2.8 Hz, 1H). ^{13}C NMR (101 MHz, CDCl$_3$) δ ppm 192.20 (d, J = 2.7 Hz), 165.82 (d, J = 257.2 Hz), 162.47 (d, J = 251.9 Hz), 149.43 (d, J = 10.2 Hz), 140.33 (d, J = 7.5 Hz), 132.70, 132.61 (m), 118.58 (d, J = 3.8 Hz), 116.49 (tt, J = 273.8, 29.0 Hz), 115.83 (d, J = 21.8 Hz), 114.87 (d, J = 22.7 Hz), 113.18 (d, J = 24.7 Hz), 107.46 (tt, J = 252.2, 40.9 Hz). ^{19}F NMR (470 MHz, CDCl$_3$) δ ppm −88.56, −104.50, −108.38, −136.89. (3-Fluoro-5-(1,1,2,2-tetrafluoroethoxy)phenyl)(4-fluorophenyl)methanone (3.3 g, 9.9 mmol) was stirred in anhydrous THF (20 mL) at rt under N$_2$. (R)-(+)-2-Methylpropane-2-sulfinamide (1.20 g, 10.0 mmol, 1.01 equiv) was added as one single portion, followed by addition of Ti(OEt)$_4$ (3.09 mL, 14.9 mmol, 1.51 equiv). The resulting solution was heated at reflux for 48 h. The cooled mixture was evaporated. H$_2$O (100 mL) was added, followed by the addition of EtOAc (100 mL). The mixture was filtered through Celite and washed with EtOAc (200 mL). The filtrate was washed with H$_2$O and brine, dried over Na$_2$SO$_4$, filtered, and concentrated to dryness. The residue was purified by silica gel flash chromatography (0−30% EtOAc in hexanes) to give **16** as yellowish viscous oil which solidified after drying under vacuum as a light yellow solid (3.50 g, yield 81.0%). LCMS (ESI) m/z 437.88 [M + H]$^+$, t_R = 3.83 min (method A). ^{1}H NMR (400 MHz, CDCl$_3$) δ ppm 7.82−6.99 (br, m, 7H), 5.90 (tt, J = 52, 4 Hz, 1H), 1.31 (s, 9H).

(R)-N-[(1R)-1-[3-Fluoro-5-(1,1,2,2-tetrafluoroethoxy)phenyl]-1-(4-fluorophenyl)-2-phenylethyl]-2-methylpropane-2-sulfinamide ((R,Rs)-17). Compound **16** (150 mg, 0.34 mmol) was stirred in anhydrous CH$_2$Cl$_2$ (7 mL) at −78 °C for 5 min under argon. BF$_3$·Et$_2$O (0.10 mL, 2.0 equiv) was added dropwise. The mixture was stirred at −78 °C for 10 min. Benzylmagnesium chloride (1.0 M in Et$_2$O, 1.4 mL, 3.0 equiv) was added slowly at −78 °C, and the resulting mixture was stirred at −78 °C for 1.5 h. The reaction mixture was quenched with saturated NH$_4$Cl and then extracted with Et$_2$O (2×). The combined organic portion was washed with H$_2$O and brine, dried over Na$_2$SO$_4$, filtered, and concentrated to dryness. The residue was purified by flash chromatography (silica gel, EtOAc/hexanes = 0−30%) to give the fast eluting fraction corresponding to (S,Rs)-**17** (29 mg); LCMS (ESI) m/z 530.36 [M + H]$^+$, t_R = 4.11 min (method A); ^{1}H NMR (400 MHz, CDCl$_3$) δ ppm 7.31−7.39 (m, 2H), 7.16−7.20 (m, 4H), 6.94−7.09 (m, 4H), 6.90 (m, 1H), 5.90 (m, 1H), 4.21 (s, 1H), 3.94 and 3.63 (ABq, J = 12.4 Hz, 2H), 1.23 (s, 9H); and the slow eluting fraction corresponding to (R,Rs)-**17** (146 mg, 81%): LCMS (ESI) m/z 530.36 [M + H]$^+$, t_R = 4.11 min (method A). ^{1}H NMR (400 MHz, CDCl$_3$) δ ppm 7.35−7.43 (m, 2H), 7.13−7.20 (m, 3H), 7.07 (t, J = 8.7 Hz, 2H), 6.93 (dd, J = 7.6, 1.8 Hz, 2H), 6.84 (d, J = 8.6 Hz, 1H), 6.70 (m, 2H), 5.85 (tt, J = 52.0, 4.0 Hz, 1H), 4.25 (s, 1H), 4.02 and 3.58 (ABq, J = 12.6 Hz, 2H), 1.20 (s, 9H). ^{13}C NMR (101 MHz, CDCl$_3$) δ ppm 162.43 (d, J = 249.0 Hz), 150.50 (d, J = 7.4 Hz), 149.17 (d, J = 11.4 Hz), 137.52 (d, J = 3.2 Hz), 134.36, 132.07, 130.96 (d, J = 8.3 Hz), 128.12, 127.20, 116.43 (tt, J = 273.2, 28.3 Hz), 116.13 (d, J = 2.9 Hz), 115.44 (d, J = 21.7 Hz), 112.44 (d, J = 23.0 Hz), 108.03 (d, J = 25.3 Hz), 107.49 (tt, J = 251.9, 41.0 Hz), 65.74, 56.51, 46.97, 22.98. ^{19}F NMR (471 MHz, MeOD) δ ppm −88.43 (m), −109.37, −113.21, −136.80 (m). The material of the slow eluting

product was crystallized from CDCl$_3$, and the single crystal X-ray structure confirmed its stereochemistry.[14]

(1*R*)-1-[3-Fluoro-5-(1,1,2,2-tetrafluoroethoxy)phenyl]-1-(4-fluorophenyl)-2-phenylethan-1-amine (18). Compound (*R*,*Rs*)-**17** (234 mg, 0.442 mmol) was stirred in 4 N HCl in a mixture of dioxane (1.5 mL) and MeOH (1.5 mL) at room temperature under Ar for 10 min. The reaction mixture was concentrated and then purified by flash chromatography (silica gel, hexanes/EtOAc) to give **18** (169 mg, 90%). LCMS (ESI) *m/z* 409.16 [M + H]$^+$, t_R = 3.26 min (method A). ^{1}H NMR (400 MHz, CD$_3$OD) δ ppm 7.29−7.50 (m, 2H), 6.87−7.22 (m, 8H), 6.77 (d, *J* = 6.15 Hz, 2H), 6.04−6.48 (m, 1 H), 3.57 (s, 2 H).

N-[(1*R*)-1-[3-(Ethenyloxy)-4-fluorophenyl]-1-[3-fluoro-5-(1,1,2,2-tetrafluoroethoxy)phenyl]-2-phenylethyl]-4-fluoro-3-(trifluoromethyl)benzamide (27). To a flame-dried, 5 L four-necked round-bottom flask equipped with a temperature controller, a mechanical stirrer, a condenser, and a N$_2$ inlet were charged Cs$_2$CO$_3$ (56.4 g, 173 mmol), 2-chloroethyl 4-methylbenzenesulfonate (64.6 g, 275 mmol), Triton X-405 (5 g), and a solution of **10a** in dry THF (1.5 L). The reaction mixture was heated to 65 °C and stirred 16 h. After cooling to 0 °C, a solution of 1 M KO-*t*-Bu in THF (787 mL) was added slowly below 7 °C over a period of 40 min. The reaction mixture was stirred below 7 °C for 6 h. Water (2 L) was added. After stirring for 10 min, the reaction mixture concentrated in vacuo to remove most of THF. It was then extracted with CH$_2$Cl$_2$ (2 × 1 L). The combined organic extracts were washed with brine (1 L) and then concentrated in vacuo to give a yellow oil, which was subjected to column chromatography using 30−50% CH$_2$Cl$_2$ in hexane to give **27** (93 g, 90%). LCMS (ESI) *m/z* 658.2 [M + H]$^+$, t_R = 4.31 min (method A). ^{1}H NMR (300 MHz, CDCl$_3$) δ ppm 7.89−7.79 (m, 2H). 7.28−7.05 (m, 5H), 6.93−6.85 (m, 5H), 6.76 (d, *J* = 5.5 Hz, 2H), 6.55 (s, 1H), 6.44 (dd, *J* = 13.9, 6.2 Hz, 1H), 5.84 (tt, *J* = 53.0, 3.0 Hz, 1H), 4.62 (dd, *J* = 13.9, 2.2 Hz, 1H), 4.39 (dd, *J* = 6.2, 2.2 Hz, 1H), 3.95 (d, *J* = 13.2, 1H), 3.77 (d, *J* = 13.2, 1H). ^{19}F NMR (471 MHz, CDCl$_3$) δ ppm −61.61 (d, *J* = 11.5 Hz), −88.25, −108.34, −108.67 (m), −132.24, −136.62 (d, *J* = 52.4 Hz). HRMS (M + H)$^+$ ESI calcd for C$_{32}$H$_{22}$F$_{10}$NO$_3$ 658.14345, found 658.14411. Orthogonal HPLC purity: 99.6%, t_R = 12.35 min (HPLC method A); 99.5%, t_R = 11.66 min (HPLC method B).

PK/PD. All animal studies were performed under the approval of the Bristol-Myers Squibb (BMS) Animal Care and Use Committee and in accordance with the American Association for Accreditation of Laboratory Animal Care (AAALAC).

In Vivo Moderate Fat-Fed Hamster Model for Assessing HDL Modulation by 10g. Male Golden Syrian hamsters (mesocricetus auratus) had been on a moderate-fat diet containing 2.5% coconut oil and 0.25% cholesterol (research diet no. 11975) for 3 weeks. Source of the animals: Charles River; VSTRACK ID 96695, ATM number 2002H009. Age and weight of the animals: upon receipt, 8 weeks old and weight is approximately 110−120 g. Upon first day of dosing, 12 weeks old and weight was approximately 160−170 g. Animals were block randomized and bled to determine baseline HDL-C. Compound **10g** (50.19 mg) was dissolved in 6.01 mL of the mixture solution composed of 100% EtOH and Cremophor (1:1). This solution was diluted 5-fold with 24.04 mL of H$_2$O to prepare a 6 mL/kg (10 mpk) dosing solution of **10g**. A dosing solution for administration of **1** was similarly prepared. Animals were dosed once a day for 3 days according to the groups (*n* = 3 for each group). Two hours after final dose, blood specimens from all hamsters were retrieved (retro-orbital puncture) and collected in 500 μL Vacutainer tubes containing K$_2$ EDTA. Animals were fasted 16 h prior to bleeding. The plasma lipid values (TG, total cholesterol, direct-HDL-C analysis) were determined using a COBAS MIRA chemistry analyzer. Plasma aliquots were also used to determine CE transfer activity and compound plasma exposures. Plasma (100 μL) from animals dosed with **10g** was fractionated using a Superose 6HR 10/30 column (GE Healthcare) attached to an AKTA purifier FPLC (GE Healthcare). Lipoproteins were eluted (0.5 mL/min) with PBS, and 300 μL fractions were collected. To determine cholesterol content, 200 μL of the cholesterol reagent and 50 μL of the fraction were mixed, and the absorbance at

500 nm was read in a spectrophotometer after 20 min incubation at 37 °C. For hamsters dosed with **1**, equal volumes of plasma from each animal were combined and the pooled plasma sample was then fractionated by FPLC and subsequently analyzed for cholesterol content.

Rat Telemetry Studies of Compound 10g on BP Effect. The study was conducted in 15 adult male Sprague−Dawley (SD) rats (∼450 g, ∼7 weeks old, fed with normal diet). These rats were implanted with a TA11PA-C40 telemetry transmitter (DSI) capable of monitoring BP, HR, and locomotor activity. The telemeterized rats (*n* = 6/group) were randomized to a vehicle group or treatment group that was dosed with compound **10g**. Three age-matched non-telemeterized satellite rats were dosed in a similar fashion as the telemetry rats to determine plasma exposures. The dose was selected to achieve ≥30 times the C_{max} observed in efficacy studies. Compound **10g** was dosed as an iv infusion in solution using 33% EtOH and 67% PEG400 as the vehicle. The dosing volume was 1 mL/kg, and the dose regimen was iv infusion of 2.5 mg/kg in the first 5 min followed by iv infusion of 5.5 mg/kg in 55 min. Arterial BP, heart rate, and gross locomotor activity were recorded continuously throughout the study period via the DSI telemetry system. Data were averaged every 10 min from continuous 36 h data recordings (12 h before and 24 h after drug) and were expressed as the mean ± SEM. Statistical comparisons were made among different treatment groups using two-factor ANOVA with Student's *t* test. Blood samples were taken at 5, 15, 30, 60, 70, and 90 min after the initiation of iv infusion from nontelemeterized satellite rats.

ASSOCIATED CONTENT

⑤ Supporting Information

The Supporting Information is available free of charge on the ACS Publications website at DOI: 10.1021/acs.jmedchem.5b01363.

> Analytical and spectral characterization data and/or experimental procedures of all the key intermediates and final compounds **7a−c, 8a,d,e, 9a,b,e−j, 10a,c,e,f,h−j**; table of solvent and addictive effects on Grignard addition of (*Rs*)-**16**, and in vitro assays (PDF)
> Molecular formula strings (CSV)

AUTHOR INFORMATION

Corresponding Author

*E-mail: jennifer.qiao@bms.com. Phone: (609) 252-7554.

Notes

The authors declare no competing financial interest.

ABBREVIATIONS USED

BP, blood pressure; CETP, cholesteryl ester transfer protein; CHD, coronary heart disease; CL, clearance; DPB, diastolic blood pressure; DPPE, diphenylpyridinylethanamine; HLM, human liver microsome; hWPA, human whole plasma assay; Lp(a), iv, intravenous lipoprotein(a); MAP, mean arterial pressure; MED, minimal efficacious dose; MEE, minimal efficacious exposure; MLM, mouse liver microsome; PL, phospholipid; PLTP, phospholipid transfer protein; RCT,

reverse cholesterol transport; SBP, systolic blood pressure; SFC, supercritical fluid chromatography; SPA, scintillation proximity assay; Tg, transgenic; TPE, triphenylethanamine; V_{dss}, volume of distribution

■ REFERENCES

(1) (a) Gordon, T.; Castelli, W. P.; Hjortland, M. C.; Kannel, W. B.; Dawber, T. R. High density lipoprotein as a protective factor against coronary heart disease. The Framingham study. *Am. J. Med.* **1977**, *62*, 707−714. (b) Drexel, H. Reducing risk by raising HDL-cholesterol: the evidence. *Eur. Heart J. Suppl.* **2006**, *8*, F23−F29. (c) Di Angelantonio, E.; Sarwar, N.; Perry, P.; Kaptoge, S.; Ray, K. K.; Thompson, A.; Wood, A. M.; Lewington, S.; Sattar, N.; Packard, C. J.; Collins, R.; Thompson, S. G.; Danesh, J. Major lipids, apolipoproteins, and risk of vascular disease. *JAMA* **2009**, *302*, 1993−2000. (d) Rhoads, G. G.; Gulbrandsen, C. L.; Kagan, A. Serum lipoproteins and coronary heart disease in a population study of Hawaii Japanese men. *N. Engl. J. Med.* **1976**, *294*, 293−298. (e) Castelli, W. P.; Garrison, R. J.; Wilson, P. W.; Abbott, R. D.; Kalousdian, S.; Kannel, W. B. Incidence of coronary heart disease and lipoprotein cholesterol levels. The Framingham Study. *JAMA* **1986**, *256*, 2835−2838. (f) Kannel, W. B. Range of serum cholesterol values in the population developing coronary artery disease. *Am. J. Cardiol.* **1995**, *76*, 69c−77c.

(2) Barter, P. J.; Brewer, H. B.; Chapman, M. J.; Hennekens, C. H.; Rader, D. J.; Tall, A. R. Cholesteryl ester transfer protein. *Arterioscler., Thromb., Vasc. Biol.* **2003**, *23*, 160−167.

(3) For recent reviews on CETP inhibitors, see the following: (a) Mantlo, N. B.; Escribano, A. Update on the discovery and development of cholesteryl ester transfer protein inhibitors for reducing residual cardiovascular risk. *J. Med. Chem.* **2014**, *57*, 1−17 and references therein. (b) Sikorski, J. A. Oral cholesteryl ester transfer protein (CETP) inhibitors: a potent approach for treating coronary artery disease. *J. Med. Chem.* **2006**, *49*, 1−22 and references therein.

(4) (a) Chapman, M. J.; LeGoff, W.; Guerin, M.; Kontush, A. Cholesteryl ester transfer protein: at the heart of the action of lipid-modulating therapy with statins, fibrates, niacin, and cholesteryl ester transfer protein inhibitors. *Eur. Heart J.* **2010**, *31*, 149−164. (b) Linsel-Nitschke, P.; Tall, A. R. HDL as a target in the treatment of atherosclerotic cardiovascular disease. *Nat. Rev. Drug Discovery* **2005**, *4*, 193−205 and references therein. (c) Briand, F.; Thieblemont, Q.; Muzotte, E.; Burr, N.; Urbain, I.; Sulpice, T.; Johns, D. G. Anacetrapib and dalcetrapib differentially alters HDL metabolism and macrophage-to-feces reverse cholesterol transport at similar levels of CETP inhibition in hamsters. *Eur. J. Pharmacol.* **2014**, *740*, 135−143.

(5) (a) Cannon, C. P.; Shah, S.; Dansky, H. M.; Davidson, M.; Brinton, E. A.; Gotto, A. M.; Stepanavage, M.; Liu, S. X.; Gibbons, P.; Ashraf, T. B.; Zafarino, J.; Mitchel, Y.; Barter, P. N. Safety of anacetrapib in patients with or at high risk for coronary heart disease. *N. Engl. J. Med.* **2010**, *363*, 2406−2415. (b) Nicholls, S. J.; Brewer, H. B.; Kastelein, J. J.; Krueger, K. A.; Wang, M. D.; Shao, M.; Hu, B.; McErlean, E.; Nissen, S. E. Effects of the CETP inhibitor evacetrapib administered as monotherapy or in combination with statins on HDL and LDL cholesterol: A randomized controlled trial. *JAMA* **2011**, *306*, 2099−2109. (c) Kathiresan, S. Will Cholesteryl Ester Transfer Protein Inhibition Succeed Primarily by Lowering Low−Density Lipoprotein Cholesterol? *J. Am. Coll. Cardiol.* **2012**, *60*, 2049−2052.

(6) (a) Berenson, A. Pfizer ends studies on drug for heart disease. *The New York Times*; The New York Times Company: New York, **2006**; Dec 3 issue. (b) Barter, P. J.; Caulfield, M.; Eriksson, M.; Grundy, S. M.; Kastelein, J. J.; Komajda, M.; Lopez-Sendon, J.; Mosca, L.; Tardif, J.-C.; Waters, D. D.; Shear, C. L.; Revkin, J. H.; Buhr, K. A.; Fisher, M. R.; Tall, A. R.; Brewer, B. Effects of torcetrapib in patients at high risk for coronary events. *N. Engl. J. Med.* **2007**, *357*, 2109−2122. (c) Tall, A. R.; Yvan-Charvet, L.; Wang, N. The failure of torcetrapib. Was it the molecule or the mechanism? *Arterioscler., Thromb., Vasc. Biol.* **2007**, *27*, 257−260. (d) Stroes, E. S. G.; Kastelein, J. J. P.; Benardeau, A.; Kuhlmann, O.; Blum, D.; Campos, L. A.; Clerc, R. G.; Niesor, E. J. Dalcetrapib: no off-target toxicity on blood pressure or on

genes related to the renin−angiotensin−aldosterone system in rats. *Br. J. Pharmacol.* **2009**, *158*, 1763−1770. (e) Hu, X.; Dietz, J. D.; Xia, C.; Knight, D. R.; Loging, W. T.; Smith, A. H.; Yuan, H.; Perry, D. A.; Keiser, J. Torcetrapib induces aldosterone and cortisol production by an intracellular calcium-mediated mechanism independently of cholesteryl ester transfer protein inhibition. *Endocrinology* **2009**, *150*, 2211−2219. (f) Forrest, M. J.; Bloomfield, D.; Briscoe, R. J.; Brown, P. N.; Cumiskey, A. M.; Ehrhart, J.; Hershey, J. C.; Keller, W. J.; Ma, X.; McPherson, H. E.; Messina, E.; Peterson, L. B.; Sharif-Rodriguez, W.; Siegl, P. K.; Sinclair, P. J.; Sparrow, C. P.; Stevenson, A. S.; Sun, S. Y.; Tsai, C.; Vargas, H.; Walker, M., III; West, S. H.; White, V.; Woltmann, R. F. Torcetrapib-induced blood pressure elevation is independent of CETP inhibition and is accompanied by increased circulating levels of aldosterone. *Br. J. Pharmacol.* **2008**, *154*, 1465−1473.

(7) Schwartz, G. G.; Olsson, A. G.; Abt, M.; Ballantyne, C. M.; Barter, P. J.; Brumm, J.; Chaitman, B. R.; Holme, I. M.; Kallend, D.; Leiter, L. A.; Leitersdorf, E.; McMurray, J. J. V.; Mundl, H.; Nicholls, S. J.; Shah, P. K.; Tardif, J.-C.; Wright, R. S. For the dal-OUTCOMES Investigators. Effects of dalcetrapib in patients with a recent acute coronary syndrome. *N. Engl. J. Med.* **2012**, *367*, 2089−2099.

(8) Publications on DPPE derivatives as CETP inhibitors: (a) Harikrishnan, L. S.; Finlay, H. J.; Qiao, J. X.; Kamau, M. G.; Jiang, J.; Wang, T. C.; Li, J.; Cooper, C. B.; Poss, M. A.; Adam, L. P.; Taylor, D. S.; Chen, A. Y. A.; Yin, X.; Sleph, P. G.; Yang, R. Z.; Sitkoff, D. F.; Galella, M. A.; Nirschl, D. S.; Van Kirk, K.; Miller, A. V.; Huang, C. S.; Chang, M.; Chen, X.-Q.; Salvati, M. E.; Wexler, R. R.; Lawrence, R. M. DiPhenylPyridylEthanamine (DPPE) derivatives as cholesteryl ester transfer protein (CETP) inhibitors. *J. Med. Chem.* **2012**, *55*, 6162−6175. (b) Miller, M. M.; Liu, Y.; Jiang, J.; Johnson, J. A.; Kamau, M.; Nirschl, D. S.; Wang, Y.; Harikrishnan, L.; Taylor, D. S.; Chen, A. Y. A.; Yin, X.; Seethala, R.; Peterson, T. L.; Zvyaga, T.; Zhang, J.; Huang, C. S.; Wexler, R. R.; Poss, M. A.; Lawrence, R. M.; Adam, L. P.; Salvati, M. E. Identification of a potent and metabolically stable series of fluorinated diphenylpyridylethanamine-based cholesteryl ester transfer protein inhibitors. *Bioorg. Med. Chem. Lett.* **2012**, *22*, 6503−6508.

(9) The SPA is an enzymatic assay in which the CETP inhibitory activity was measured as the amount of [^{3}H]cholesteryl ester ([^{3}H]CE) transferred from HDL ([^{3}H]CE/HDL) to biotinylated LDL and captured on avidin-SPA beads. See ref 8a and Supporting Information for assay details.

(10) For the transgenic mouse pharmacodynamic study, transgenic mice expressing human CETP and apoB-100 were used. Predose blood samples were collected by retro-orbital bleed. Compounds were formulated in ethanol/Cremophor/water at a 1:1:8 ratio and dosed at 10 mg/kg, po. At 2, 4, and 8 h after dosing, blood samples were collected. Cholesterol ester transfer activity was measured in all blood samples and normalized by the activity measured in the same animal at baseline (mean of four or five mice per dose).

(11) For the hamster study, plasma HDL-C was measured in male Golden Syrian hamsters initially fed a moderately fat diet (2.5% coconut oil, 0.25% cholesterol) for 2 weeks. The hamsters were then dosed with vehicle or compound, po, q.d. At 2 h after dosing on day 3, plasma samples were obtained and HDL-C was measured and compared to the values measured before dosing.

(12) Wang, T. C.; Qiao, J. X.; Chen, A. Y.; Taylor, D. S.; Yang, R. Z.; Paul, G.; Sleph, P. S.; Li, J. P.; Li, D.; Chang, M.; Chen, X.-Q.; Li, J.; Levesque, P.; Huang, C. S.; Adam, L. P.; Salvati, M. E.; Finlay, H.; Wexler. R. R. Discovery and synthesis of triphenylethanamine derivatives as highly potent cholesteryl ester transfer protein inhibitors. *Abstracts of Papers*, 249th National Meeting and Exposition of the American Chemical Society, Denver, CO, U.S., March 22−26, 2015; American Chemical Society: Washington, DC, 2015; MEDI-78.

(13) (a) Kamau, M. G.; Harikrishnan, L. S.; Finlay, H. J.; Qiao, J. X.; Jiang, J.; Poss, M. A.; Salvati, M. E.; Wexler, R. R.; Lawrence, R. M. Synthesis of tertiary carbinamines. *Tetrahedron* **2012**, *68*, 2696−2703. (b) Shaw, A. W.; deSolms, S. J. Asymmetric synthesis of α,α-diaryl and

α-aryl-α-heteroaryl alkylamines by organometallic additions to *N-tert*-butanesulfinyl ketimines. *Tetrahedron Lett.* **2001**, *42*, 7173−7176.

(14) (a) Davis, F. A.; McCoull, W. Concise asymmetric synthesis of α-amino acid derivatives from *N*-sulfinylimino esters. *J. Org. Chem.* **1999**, *64*, 3396−3397. (b) Davis, F. A.; Reddy, R. E.; Szewczyk, J. M.; Reddy, G. V.; Portonovo, P. S.; Zhang, H.; Fanelli, D.; Reddy, R. T.; Zhou, P.; Carroll, P. J. Asymmetric synthesis and properties of sulfinimines (thiooxime *S*-oxides). *J. Org. Chem.* **1997**, *62*, 2555−2563. (c) Ellman, J. A. Applications of *tert*-butanesulfinamide in the asymmetric synthesis of amines. *Pure Appl. Chem.* **2003**, *75*, 39−46 and references therein.

(15) Full crystallographic data have been deposited with the Cambridge Crystallographic Data Center under CCDC reference number 1422275. Copies of the data can be obtained free of charge via the Internet at http://www.ccdc.cam.ac.uk.

(16) Li, J.; Smith, D.; Qiao, J. X.; Huang, S.; Krishnananthan, S.; Wong, H. S.; Salvati, M. E.; Balasubramanian, B. N.; Chen, B.-C. Preparation of monofluorophenols via the reaction of difluorobenzene derivatives with potassium trimethylsilanoate. *Synlett* **2009**, *2009* (4), 633−637.

(17) Li, J.; Qiao, J. X.; Smith, D.; Chen, B.-C.; Salvati, M. E.; Roberge, J. Y.; Balasubramanian, B. N. A practical synthesis of aryl tetrafluoroethyl ethers via the improved reaction of phenols with 1,2-dibromotetrafluoroethane. *Tetrahedron Lett.* **2007**, *48*, 7516−7519.

(18) (a) McKinley, N. F.; O'Shea, D. F. Efficient synthesis of aryl vinyl ethers exploiting 2,4,6-trivinylcyclotriboroxane as a vinylboronic acid equivalent. *J. Org. Chem.* **2004**, *69*, 5087−5092. (b) Okimoto, Y.; Sakaguchi, S.; Ishii, Y. Development of a highly efficient catalytic method for synthesis of vinyl ethers. *J. Am. Chem. Soc.* **2002**, *124*, 1590−1591.

(19) CETP facilitates the removal of cholesteryl esters (CE) from HDL and thus reduces HDL-C levels, while PLTP promotes the transfer of phospholipids (PL) from triglyceride-rich lipoproteins into HDL and increases HDL-C levels. PLTP activity was measured as described previously (*J. Clin. Invest.* **1999**, *103*, 907−914) with modifications. See Supporting Information for more details.

(20) Lipoprotein disruption assay: Lipoprotein disruption components (human origin, Biomedical Technologies, Inc.) were diluted in assay buffer [50 mM HEPEs (pH 7.4), 150 mM NaCl, 0.05% NaN_3 (w/v)] to concentrations utilized in the aforementioned SPA assay. LDL and HDL were diluted to 5 and 16 μg/mL, respectively. In-house generated [^{3}H]cholesterol ester-HDL was diluted 30-fold in the reaction mix which was subsequently incubated in the absence and presence of CETP inhibitors for 4 h at 37 °C. Lipoprotein associated [^{3}H]cholesterol ester was resolved by agarose gel electrophoresis and imaged by quantitative phosphor imaging autoradiography.

(21) Tg WPA: Measurement of cholesterol ester transfer activity in plasma samples obtained from compound-treated human CETP/apoB100 dual transgenic mice (Taconic Laboratories) was obtained following the described variation of the hWPA methodology. See Supporting Information for details.

(22) Lloyd, D. B.; Lira, M. E.; Wood, L. S.; Durham, L. K.; Freeman, T. B.; Preston, G. M.; Qiu, X.; Sugarman, E.; Bonnette, P.; Lanzetti, A.; Milos, P. M.; Thompson, J. F. Cholesteryl ester transfer protein variants have differential stability but uniform inhibition by torcetrapib. *J. Biol. Chem.* **2005**, *280*, 14918−14922.

(23) A survey of the literature reports from 1950 to 2004 on BP studies in different animal species showed that rats were the most widely used animal species for preclinical BP study. It is believed that common mechanisms might affect BP in rats and humans and it might be predictive for BP effects in human. In our in-house telemeterized mice studies, BP and HR effects of various known clinical agents were reproduced in telemetry rats at clinically relevant doses/exposures; sensitivity to detect ≥5−10% changes.